Allyne Machado dos Santos

Modelling, Control, and Optimization of a Recirculating Aquaculture System

Thesis for the degree of Philosophiae Doctor
Trondheim, October 2023

Norwegian University of Science and Technology
Faculty of Natural Sciences
Department of Chemical Engineering

NTNU
Norwegian University of Science and Technology

Thesis for the degree of Philosophiae Doctor

Faculty of Natural Sciences
Department of Chemical Engineering

ISBN 978-82-326-7372-8 (printed version)
ISBN 978-82-326-7371-1 (electronic version)
ISSN 1503-8181

Doctoral theses at NTNU, 2023:336

Printed by NTNU Grafic Center

To my parents and my beloved fiancée

Summary

Recirculating aquaculture systems (RAS) are closed-loop systems that recycle most of the effluent of a fish tank after particle removal and water treatment. This type of process requires good control of the water quality, as the carbon dioxide, ammonia, and nitrate concentrations are toxic for the Atlantic salmon (*Salmo salar* - fish species considered) when above certain values, and oxygen concentration needs to be in a certain range to the welfare of the fish. Due to the recycling, some of those concentrations are handled by the water treatment units, such as CO_2 stripper, and biofilter, which transforms ammonia into nitrate. The accumulation of nitrate explains the necessity of water exchange, *i.e.*, some of the recycling water is purged while the makeup of fresh/brackish water is done.

To regulate these quantities into an optimal value considering the process constraints and fish requirements, simplified steady-state and dynamic models were developed, and validated with real data. The developed models include pH modelling, which is an important variable in the system due to its effect on carbon dioxide and ammonia concentrations, so it should be monitored and controlled. The process was optimized using fish requirements for water quality only, but the optimization problem was reformulated considering fish growth effect on the water quality, and other real-life limitations, considering higher minimum recirculation flow rate due to the risk of sedimentation in pipes and fish swimming requirements.

Water quality monitoring can be challenging due to the lack of the correct sensors in the RAS facility. In these cases, the monitoring is done every now and then by taking samples and analyzing them in a laboratory. The lab measurements can differ a lot from reality, depending on the magnitude of the measured variable and the precision of the equipment. Another issue is that the measurements take time to be taken, adding a large gap between samples. The frequency of monitoring is crucial to a RAS process, as one mistake can put all the fish dead. To mitigate these issues with lab measurements, an automatic search for a soft sensor was applied to the developed RAS model. The search tool, named Auto-keras, did not find a good feedforward neural network that would take the steady-state trend in the input features and predict well CO_2, NH_3, and NH_4^+ concentrations. This

might be due to the lack of information on the input features, *i.e.*, large variability of the output variables.

The results of this thesis show that the developed RAS model is sensitive to fish metabolism, which was considered to produce constant quantities of carbon dioxide and ammonia. In addition, the model showed numerical robustness and good performance in monitoring, controlling, and optimizing the process.

Acknowledgements

I would like to thank my supervisor, Prof. Sigurd Skogestad, for giving me the honor of being his student, and for the dedication, patience, support, and all the knowledge shared during this journey that was this PhD and during my internship while I was still pursuing a master's degree. I would like to thank also my co-supervisors, Assoc. Prof. Kari Attramadal for all the knowledge and experience shared about the process, and Prof. Johannes Jäschke for the pieces of advice and support.

I would like to thank the PhD evaluation committee, Prof. Torstein Wik, Dr. Sveinung Johan Ohrem, and Assoc. Prof. Idelfonso B. R. Nogueira, for taking the time to read this thesis, even in a record time, and for their extremely valuable feedback.

I thank my former project and master students for contributing to this work, Hege Landbø, Kristin Ø. Madsen, Ida Havnen, Mari H. Bøhleng, Kristin Andersskog, Khanh Hoang, and Espen Karlsen. It was great to participate in their academic development.

Being here in Trondheim was the best thing that ever happened to me, I am truly grateful. I value not only the opportunity of studying overseas, but also the changes in perspective, and personal growth. Trondheim will always be in my heart, just beside the brilliant people I got to know because I was here. I am also grateful for the best flatmate I could have ever asked for, Lucas Bernardino, with whom I enjoyed very much working and spending lots of time, especially on all the game nights with Otávio and Fabiana. All of you are a blessing in life, and everything I say will not express my gratitude enough. This extends to the Brazilian gang, Carol, José Otávio, Aline, Andressa, Leonardo, and Bonita for all the barbecues by the river and doing groceries together, especially during the homesick times.

I also want to thank my colleagues from the Process Systems Engineering group, Andrea, Fabienne, Bahareh, Haackon, Mandar, Cristina, Adriaen, Dinesh, Timur, David, Halvor, Evren, Zawadi, Risvan, Simen, Robert, and Lucas Camman, for the discussions during lunch, happy hours, and ski travels.

I thank my parents, who did everything to make me capable of achieving this. I thank them for their support and happiness from all times, especially since the first opportunity I had to come to Trondheim during my internship.

Finally, I thank my fiancée for embracing this long-distance relationship for the sake of this PhD. All the care and happiness from so far away were very important to me, giving me hope and strength to keep on going.

Allyne M. dos Santos
Trondheim, October 2023

Contents

List of Figures

List of Tables

Chapter 1

Introduction

1.1 Motivation and Scope of the thesis

Aquaculture is a general term for breeding, rearing, and harvesting aquatic animals. Some species of these aquatic animals are easier or more economically appealing to be reared than others. From more than five hundred species commercially farmed, Atlantic Salmon is one of the most profitable species. Compared to other types of livestock, aquaculture provides a more environmentally friendly solution, as it uses fewer water resources.

Over the past four years, COVID-19 has been disseminated across the continents to the point it alerted the world of its deadly potential and countries started to restrict their borders. With that, the exports of agri-food faced difficulties, inhibiting trades of fish, in particular. In addition, the pandemic reduced the number of workers, supplies, and availability of new animals. Besides all the impacts in every step of the production chain, aquaculture has managed to grow, despite being at a much lower pace than before the pandemic (FAO, 2022).

There are a lot of types of aquaculture, which are described in the next chapter. This thesis focuses on modelling one of them, a recirculating aquaculture system of Atlantic Salmon (*Salmo Salar*), on the application of a methodology for control structures design to this type of system, and on the application of a feedforward neural network to predict the main water quality parameters.

The Recirculating aquaculture system is a technology that includes complex and interdependent systems. Modelling this technology is a hard task and a trade-off should made between accuracy and computational time. The more detailed the model, the more close to reality it is when simulating RAS. On the other hand, to develop a good performance control, the more complex the model is, the longer it takes to generate one sample or not even that (when there are numerical issues). As time is a crucial variable in advanced control, frequently one needs to decrease the

complexity of the model for its use to be feasible. This research mainly focused on developing simplified models (as simple as possible) for simulation and control purposes.

This work is a collaboration with Nofitech, a company that designs and provides recirculating aquaculture systems (RAS) for freshwater or seawater operation, for smolt or higher phases of fish life-cycle. The system that this contribution is about is the land-based design that they already have. The main objective of this collaboration is to develop a model for pH, CO_2, and alkalinity control in recirculating aquaculture systems. The specific objectives are to study the effects of placement of pH and alkalinity adjustments; predict the behavior of the system in the main compartments (fish tank, bio-filter, and stripper); use the model for production optimization and control, including a study of different control structures, such as nonlinear model-based predictive control, economic nonlinear model-based predictive control, and proportional integral control with real-time optimization on top; and study the application of a feedforward neural network as a surrogate model to predict carbon dioxide, ammonia, and ammonium.

1.2 Research Contribution and the Thesis Structure

The thesis is organized in a paper-based format with seven chapters. Chapter 1 introduced the motivation and the objectives of this thesis. The other chapters present the research contributions developed during this PhD work and are described below.

- **Chapter 2** introduces the necessary background knowledge for the reader to understand the fish farming categories.
- **Chapter 3** contains the detailed RAS process description studied in this thesis and the development of the RAS model for optimization and control.
- **Chapter 4** formulates the optimization problem for RAS and compares three optimization control structures, *i.e.*, economic model predictive control, model predictive control, and proportional integral controls with real-time optimization on top.
- **Chapter 5** reformulates the optimization problem for RAS with realistic constraints on the water flow rate and CO_2 exposure.
- **Chapter 6** introduces a surrogate model for CO_2, ammonia, and ammonium concentrations to complement the lab-based monitoring of these quantities.
- **Chapter 7** summarizes this thesis and presents suggestions for future work.

1.3 List of Publications

1.3.1 Reviewed Conference Papers (Norwegian publication level 1)

- A. M. dos Santos, K. J. K. Attramadal, S. Skogestad. Optimal Control of Water Quality in a Recirculating Aquaculture System (13th IFAC Symposium on Dynamics and Control of Process Systems, including Biosystems (DYCOPS), Busan, South Korea). *IFAC-PapersOnLine*. v. 55(7) , pp 328-333, Elsevier, 2022. - **Chapter** 4

- A. M. dos Santos, E. Karlsen, S. Skogestad, K. J. K. Attramadal. Soft Sensor of Key Components in Recirculating Aquaculture Systems, using Feedforward Networks (32nd European Symposium on Computer Aided Process Engineering (ESCAPE), Toulouse, France). *Computer Aided Chemical Engineering*. v. 51, pp 1495-1500, Elsevier, 2022. - **Chapter** 6

1.3.2 Journal paper (Norwegian publication level 1)

A. M. dos Santos, L. F. Bernardino, K. J. K. Attramadal, S. Skogestad. Steady-state and dynamic model for recirculating aquaculture systems with pH included. *Aquacultural Engineering*. v. 102, 102346 (14 pages), 2023. - **Chapter** 3

1.3.3 Paper published during my Ph.D. studies, but not included in this thesis

M. J. C. Díaz Arias, A. M. dos Santos, E. Altamiranda. Evolutionary Algorithm to Support Field Architecture Scenario Screening Automation and Optimization Using Decentralized Subsea Processing Modules. Processes. v. 9, no. 1, pp. 184, 2021. https://doi.org/10.3390/pr9010184

1.4 List of Presentations and Poster Contributions at Conferences

- A. M. dos Santos. Conference presentation at Computer Aided Process Engineering FORUM (CAPE forum), online, 2020: "Surrogate Optimizer using Machine Learning Techniques" - Applied to a heat exchanger network.

- A. M. dos Santos. Conference presentation at Nordic Process Control Workshop (NPCW), Luleå, Sweden, 2022: "Optimal Control of Water Quality in a Recirculating Aquaculture System"

Chapter 2

Background

Fish farming is quite an old technique for complementing the food source of the surrounding population. It is unknown exactly when it began, but it is speculated to have begun before 2000 b.c. in China, with the common carp (*Cyprinus carpio*) aquaculture (Rabanal, 1988). Fish aquaculture's popularity increased a lot in the 1950s when they started to produce and hatch fish eggs to produce fry instead of acquiring them from nature.

2.1 Fish farming processes

Rearing fish in a contained environment can be classified according to their location, type of enclosure, fish food source, water disposal, and intensity of human intervention. This section points out the main differences between these types, but more details and other aquaculture systems can be found, for example, in the book authored by Tidwell (2012).

2.1.1 Land-based vs offshore farming

Offshore farming consists of an enclosure that, despite keeping the fish growing in a limited volume, enables the water to circulate easily between the inside and outside of the caged water volume. The most common examples of offshore fish farming are net pens, where the enclosure is made of nets, and closed cages, where the seawater does not flow freely, but a lot easier than land-based farming, see Figure 2.1. The disadvantages of net pens are the escaping of fish, higher exposure to sea lice, thus pathogenic bacteria, and accelerated contamination due to the high density of fish per volume unit. A solution to sea lice exposure and the potential risk of an epidemic is locating the net pens far away

from the wild fish (Frazer, 2009). Another solution to the exposure is closed cages, when there is seawater treatment of the inlet and outlet streams.

Figure 2.1: A typical closed cage (BLUEGREEN GROUP, 2022).

In the case of Atlantic salmon, usually they are reared in land-based farms until smoltification. After that, they are transferred to sea cages to grow until market size. Recently, there has been much attention to growing smolts and post-smolts in land-based farms, *i.e.*, extending the time period of the land-based farm phase. Therefore, studies about process modelling of smolt or post-smolt phases are important to reduce the time the fish spend in sea cages and being exposed to sea lice, and other diseases.

Land-based fish farming can rear single or multiple species. In case it is multiple species, it is usually done in nature, such as aquaponics, and organic aquaculture (Lembo and Mente, 2019), as in ponds with a small ecosystem, rivers, or estuaries, while single-species farming is usually done in raceway tanks (see Figure 2.2) or in large tanks in an industrial facility, which is the focus of this work.

2.1.2 Extensive vs intensive farming

There is an extensive type of aquaculture where the fish food source is cultivated along with the fish, while an intensive type relies completely on an external food source. There are also semi-intensive farms, which consist of the partial feeding of the fish from an external source when only an internal source is

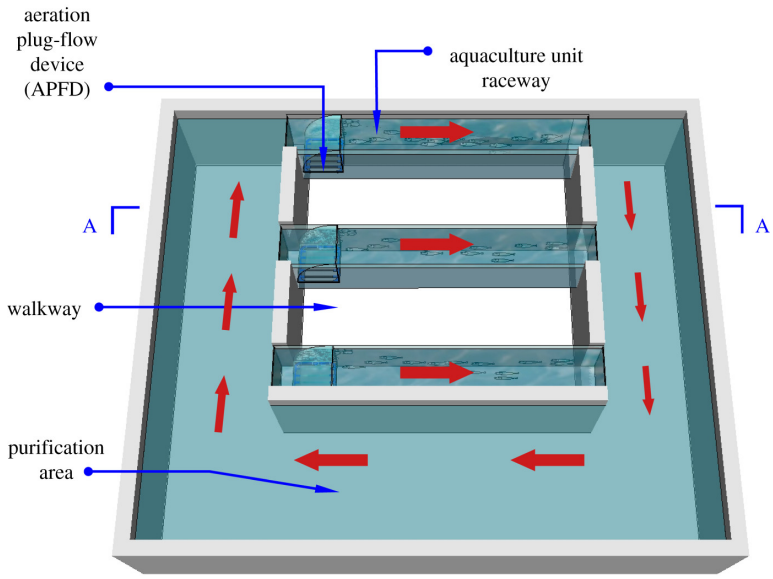

Figure 2.2: A typical raceway with water and solid treatment systems (Li et al., 2019).

not enough for farming purposes. The external food source provides controlled diet food specifically developed to optimize fish performance and welfare. Commercial providers usually indicate the daily portion size, although it does not remove the necessity of feed control, as fish hunger may vary with water conditions, lighting, and diseases.

To ensure fish performance, feeding must be controlled. Farheen et al. (2018) developed an app connected with a feeding control so one can receive alerts for feeder system malfunction, set a feeding schedule, and monitor fish tank conditions with the aid of a camera. Even though it has an automatic alert, one still needs to use their experience to make a decision over the feeding system. An even more automated system was proposed by Liu et al. (2014). The authors proposed a computer-vision method for measuring the feeding activity of Atlantic salmon from a RAS facility, accounting for fish overlaps and water surface reflections. They also validated their method by comparing their results with manual observation.

There is also the possibility to mix extensive and intensive farming. Villar-Navarro et al. (2021) developed experiments on the use of microalgae biotechnology to remove nitrogen and phosphorous from recirculating aquaculture systems (RAS) effluent, while generating fish feed additive and fish meal substitute. This type of process is called semi-intensive farming.

2.1.3 Water circulation

In land-based intensive farming, the effluent is more accounted for in terms of environmental impact. With the evolution of environmental laws, the regulation of these types of processes also evolved, pushing the aquaculture industry to reduce its environmental impact.

The quality of the effluent has received a lot of attention, which has led to the development of a more complex treatment process with less environmental impact. Along that line, part of the treated water can be recirculated or even reused entirely in the process. When there is no water recirculation, the land-based intensive system simply consists of flow-through systems with water discharge to nature or to a sewage system. When most of the effluent is treated and recirculated, and the rearing environment is fully controlled, the land-based intensive system is called a recirculating aquaculture system.

2.2 RAS process

Recirculating aquaculture systems are closed-loop systems that combine physical, chemical, and biological processes to rear a single species of fish. In this type of process, almost all of the water used is treated and recycled within the system. This characteristic enables the industry to build a controlled environment in the operating conditions that satisfy the fish while generating almost no environmental impact and waste. The RAS process, illustrated in Figure 2.3, consists of fish tanks, water, and solid treatment systems, and has several advantages, such as no losses of fish escaping, less contact with external pathogens, controlled rearing conditions, and is more sustainable.

RAS offers several advantages over traditional open systems, including improved water efficiency, reduced environmental impact, and better control over the growth and health of aquatic animals. By reusing the water, RAS can reduce the amount of water needed for fish farming by up to 90% compared to traditional open systems. Additionally, RAS can reduce the need for antibiotics and other chemicals, as the closed-loop system helps to prevent disease outbreaks and keeps the water quality consistent.

RAS can be designed to operate on a small scale, such as in a backyard garden, or on a commercial scale, such as in a large fish farm. The system is highly flexible, and the design can be tailored to meet the specific needs of the species being farmed. The key to successful RAS operation is maintaining consistent water quality parameters, including temperature, pH, dissolved oxygen, and ammonia and nitrite levels. This is achieved through a combination of solids removal and water treatment systems. Water is recirculated through the system

continuously, with only a small percentage of water replaced to account for losses due to evaporation and waste removal.

Figure 2.3: A typical industry facility of RAS (Hatchery - Feed & Management, 2020).

2.2.1 Fish tank

The fish tank geometry is a result of studies to reduce cost and manage risk, by reducing the need for human interaction and reducing contact between different fish populations, which can increase the probability of spreading diseases. These issues can be avoided with larger tanks, but it also adds other types of problems, such as difficulty in fishing the ones from the bottom. Summerfelt et al. (2016) compiled a survey on large circular and octagonal tanks to aid the development of a computational fluid dynamics (CFD) model to study what affects water rotational velocities and mixing in such large tanks.

2.2.2 Solids removal system

The solids removal system is crucial to water recirculation. It consists of mechanical unit operations to remove solid particulate matter. Cripps and Bergheim (2000) did an extensive review on solids removal and management in flow-through and recirculating systems. The authors described how the efficiency of the solids management system can be increased with a pre-treatment phase, which is the increasing of the solids concentration of the effluent, and also described several types of solids removal systems. Summerfelt and Penne (2005) studied how important is to add an inline sedimentation unit to remove heavy solids before the drum filter, so its load is reduced, thus, avoiding equipment failure.

2.2.3 Water treatment system

The water treatment system's goals are to eliminate or control substances that are toxic to the fish, add oxygen, and reduce freshwater usage. The main units consist of the biological treatment of ammonia and organic matter produced by the fish, the stripper, that removes CO_2 that can accumulate in the water, preventing pH levels from becoming too low, and oxygen makeup. Some other units can also be present, such as denitrification, ozonation, and UV units. A denitrification unit can be added to the system to transform nitrate into nitrogen, and ozonation or UV units are implemented to guarantee disinfection of the recirculating water.

2.2.4 Challenges of a RAS process

The major challenge for RAS is the financial aspects, followed by the difficulty in obtaining more reliable and useful data, and system failures due to instability or equipment malfunction. The cost of implementing a RAS process can be a significant barrier to entry for smaller-scale farmers.

To obtain more reliable data, the RAS process companies need to invest more in sensors and artificial intelligence technology to visualize fish performance so they can be used in advanced control structures and improve the level of automation. The major contribution of this thesis consists of developing a model to reach this next level and avoid system instability with a robust control structure, promoting fish welfare and high performance.

2.3 Modelling RAS and its challenges

There are a lot of challenges when modelling an intensive fish farming process, such as the adaptable behavior of the Atlantic Salmon. Beyond the change of optimal required conditions throughout its early stage in life, some types of experience can affect the fish for its entire life cycle. Despite this species' ability to adapt to slight changes in pH, temperature, lighting, and salinity conditions, if exposed to a certain level of carbon dioxide, ammonia, and nitrate, the growth performance and welfare of the fish decreases (Thorarensen and Farrell, 2011).

Ammonia and nitrite are toxic compounds that can build up in RAS as a result of fish waste and uneaten feed. Ammonia and nitrite levels must be monitored and controlled through the use of biofiltration or chemical treatments. Davidson et al. (2017) evaluated the performance of post-smolt Atlantic salmon in RAS to two levels of exposure to nitrate. They concluded that a nitrate concentration higher than 100 mg/L starts to affect post-smolt Atlantic Salmon performance and welfare.

Carbon dioxide toxicity is a concern in RAS and can impact the health and growth of Atlantic salmon. The tolerance of Atlantic salmon to elevated CO_2 levels varies depending on factors such as fish size, life stage, and duration of exposure. Mota et al. (2019) studied the effect of CO_2 on growth, welfare, and health, and concluded that increasing CO_2 concentration in the water decreases linearly and significantly growth of post-smolt Atlantic Salmon. Khan et al. (2018) went further and studied the effect of acute and long-term exposure to CO_2, which is a type of experience that affects the fish for life.

There are several types of modelling that can be used to study and design RAS. Among the most frequently used types are:

1. Hydrodynamic modelling: this approach simulates water flow within the RAS. It aids in predicting water movement, treatment processes, distribution to different tanks, and its return to the aquatic species.

2. Water quality modelling: this method forecasts changes in water quality within the RAS. It assesses how different water treatment technologies impact water quality and the effects on the health of aquatic organisms.

3. Biological modelling: this type is used to simulate the growth and behavior of fish within RAS. It helps predict how varying conditions, feeding strategies, and stocking densities influence the growth and welfare of the aquatic species.

4. System dynamics modelling: This holistic modelling approach considers the entire RAS system, examining interactions between subsystems such as water treatment, fish cultivation, and energy generation. It aids in comprehending overall system performance and identifies areas for potential enhancement or optimization.

There is no model that reflects all types of subsystems in RAS reality so far. The difficulty lies in integrating a water treatment model with fish growth and solid treatment models while considering all effects among them, and water quality requirements for the fish. Besides that, there is a large possibility that the integration of all models would lead to a too complex model to be suitable for optimization and control.

For this purpose, modelling each part of the RAS process and controlling it separately might not lead to a global optimum, but it can still be beneficial by generating stability and improvements.

Modelling a process has several types of levels regarding the amount of detail and known behavior. It can be based purely on experimental data, as an empirical model, based on material and energy balances, or even a mixture of both.

Depending on the assumptions, the level of detail can increase a lot the complexity of the model, creating a barrier to good control of the operating conditions. The aim of this work is to develop a simplified model, *i.e.*, a model that is simple, with empirical equations to simplify what is reasonable to simplify, but also with physical equations to model the chemical unit operations, and use this model to develop and compare optimal control structures.

Barbu et al. (2016) developed a model for the trickling biofilter, and used it to control water level, oxygen concentration, and pH after the mechanical filter in a pilot RAS plant rearing carp. In this case, the authors used acid and base to control pH and the pH response varied from 2 to 12. Colt et al. (2012a) developed carbon dioxide transfer models based on existing oxygen models and they also verified the models for stripping data in a further study (Colt et al., 2012b). This type of model was validated with experimental data, but its complexity and existence of a single solution were not evaluated for process control purposes, which becomes a suggestion for future work.

Wik et al. (2009) developed a model integrating water treatment and fish growth models, but they did not explicitly model the pH, which is a very important variable that affects ammonia and carbon dioxide levels, which, as mentioned already, are toxic for the fish when above certain values. Another issue was the numerical problems, challenging its usage for process optimization and control. Pedersen and Wik (2020) improved the previous model solving the numerical issues and adding new features, such as the denitrification process and consideration of energy balances. The lack of a model that can represent a certain stage of the process is necessary to reach the next level of automation in RAS.

The pH level of the water is another important aspect of water quality control in RAS. Fish have specific pH requirements, and pH levels that are too high or too low can be harmful. RAS typically uses pH adjustment systems to maintain the desired pH level. By including pH in the model and assuming a stage in the fish's life where their metabolism is constant, we can simplify it by assuming that the amount of feeding is exactly what they need and that there will not be leftovers. These assumptions are definitely not close to reality during the fry and juvenile stages, but during the smolt and post-smolt stages, these assumptions are reasonable. Not considering feed accumulation or starvation means that the fish are satisfied with the feeding, *i.e.*, the fish metabolism is fairly constant if they are in optimal feeding conditions with clean and oxygenated water. Therefore, we assume that feeding and oxygen control have good performance.

The present thesis is focused on developing and using a simplified model with pH included to optimize and control water conditions. The development of the model is described in detail in Chapter 3, while the optimization and control are presented in Chapters 4 and 5.

Chapter 3

Steady-state and Dynamic Modelling of Water Quality

This chapter presents the development of the steady-state and dynamic models of Recirculating Aquaculture Systems for control and optimization purposes. The chapter is very similar to Paper I, which was published in the Aquacultural Engineering journal.

3.1 Abstract

In this work, simplified steady-state and dynamic models of a Recirculating Aquaculture System (RAS) of Atlantic salmon (*Salmo salar*) are described. The RAS process under study includes a fish tank, a biofilter, a CO_2 stripper, and an oxygen cone. Compared to existing models, the main contribution is that it explicitly models the pH, by using reaction invariants such as total inorganic carbon (TIC), total ammonia nitrogen (TAN), and alkalinity. As the possibility of placing the pH/alkalinity adjustment (base or buffer addition) into the fish tank or into the biofilter was considered, four steady-state scenarios were studied, where one of the adjustments is utilized in each scenario. A dynamic simulation of the process with oxygen and pH controllers was performed and compared with commercial RAS production data, and what adjustments had to be done to get an agreement between the model and the plant data.

3.2 Introduction

Fish aquaculture involves the use of large tanks filled with freshwater or saltwater to cultivate fish. As the global demand for food continues to grow, the

Food and Agriculture Organization of the United Nations (FAO) has recognized aquaculture as a promising source of food to meet this demand (FAO, 2020).

Atlantic salmon undergo freshwater stages until they reach a mature smolt size, after which they are transferred to net pens during the post-smolt phase and continue to grow until they reach market size (Global Salmon Initiative, 2020). Expanding the inland phase of aquaculture has several advantages, including reducing fish losses from escapes, lowering the probability of diseases due to the absence of contact with external pathogens, and the ability to provide controlled rearing conditions with vaccinations. However, the main disadvantage is that as the fish grow, they require more space and may need to be spread across multiple tanks or transferred to larger tanks.

The current types of configuration of recirculating aquaculture systems (RAS) show room for improvement, as they are not operated optimally and are not fully automated, i.e., they are operated manually to preserve satisfactory conditions for the welfare of the fish.

Carbon dioxide (CO_2), ammonia (NH_3), and nitrate (NO_3^-) can be toxic for fish above certain levels (Bergheim and Fivelstad, 2014; Davidson et al., 2017; Mota et al., 2019), and maintaining an acceptable pH level is also crucial. In industrial setups, CO_2 and NH_3 levels are typically monitored indirectly by measuring the concentrations of total inorganic carbon (TIC), total ammonia nitrogen (TAN), and alkalinity. These concentrations remain reaction invariant with respect to pH and the equilibrium reactions that occur during this process, meaning that their concentrations do not change when pH or the concentration of any component involved in the equilibrium reactions fluctuates.

It is possible to develop a dynamic model for these quantities without explicitly including pH in the model by using reaction-invariant quantities, such as TIC, TAN, and alkalinity. Examples of such models can be found in the RAS model developed by Wik et al. (2009) and the model extended by Pedersen and Wik (2020). Both models include fish and bacteria metabolisms, with Pedersen and Wik (2020) extending the model by including a model for the stripper. However, neither model considers the effect of pH explicitly, as it is not necessary when using reaction-invariant quantities.

To our knowledge, no dynamic models for RAS that consider the effect of pH have been published in the literature. One approach to include pH in the model is to use dynamic balances for all components, including the H^+ concentration, and use the extent of reactions as static coupling variables. However, an alternative approach that uses reaction-invariant variables and fewer differential equations, as proposed for pH systems since the 1980s (Gustafsson and Waller, 1983), may be preferable due to numerical reasons. In this study, we test both approaches and show how the reaction-invariant approach is more suitable.

In this paper, we present simple steady-state and dynamic models that are suitable for controlling and optimizing the design of a RAS (from Nofitech). Our main objective was to develop a water quality model for the main units (fish tank, biofilter, and stripper) that also includes pH, and to study the effects of the placement of substances to adjust pH and alkalinity.

3.3 Process Description

3.3.1 Process overview

The recirculating aquaculture system is composed of a fish tank and a water treatment system, which includes a biofilter and a CO_2 stripper. Solid removal from the fish tank is also present, but for simplicity, solids are not included in our model. Additionally, denitrifying and disinfection units could be present in other configurations of RAS, but the RAS being studied does not have these types of equipment. An illustration of the process is shown in Figure 3.1.

The fish tank receives two inlet streams, one containing fish feed in the form of solid pellets and the other containing recirculated water enriched with oxygen. Fish metabolism takes place in the tank, as described by reaction (3.1). The effluent water from the fish tank is then sent to the biofilter, where a small amount of makeup water is added. In the biofilter, bacteria convert ammonium into nitrate, as described by reaction (3.2), with an assumed conversion efficiency of 97% of TAN. The effluent from the biofilter is then sent to a CO_2 stripper, where CO_2 is removed with an efficiency of around 60%-70%. To avoid the accumulation of nitrate and other compounds, a purge stream is taken out after the stripper. The remaining recycled water is then fed back to the fish tank after oxygen has been added using an oxygen cone. In Figure 3.1, the red lines indicate the four options for pH correction, which can be done in the fish tank (T) and/or in the biofilter (B) by adding base (NaOH) or buffer ($NaHCO_3$). Although buffer can be used for pH correction, it also adds bicarbonate to the system, making it more difficult to keep low CO_2 levels. Therefore, it is not clear which one should be used. Additionally, we assume that there is a possibility of adding pH correction in the fish tank, which might not be common practice due to associated risks. However, we assume that the fish farm is knowledgeable about handling this matter and has the power to mitigate any risks.

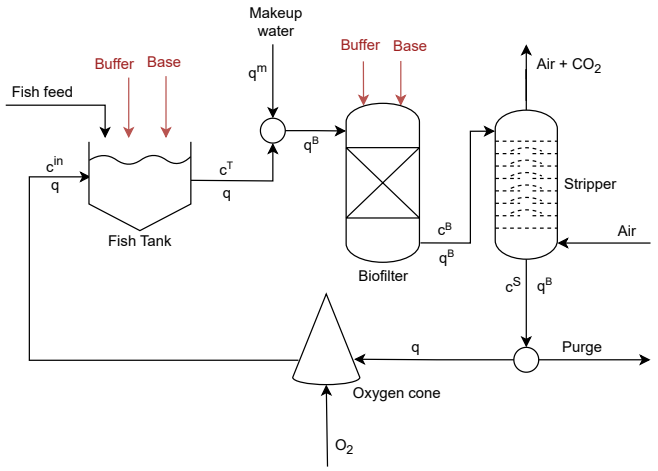

Figure 3.1: Flowsheet for RAS process studied in this paper with 4 optional base and buffer intakes (in red lines).

3.3.2 Chemical reactions

In this work, we only focus on modelling the water system of the fish tank and assume that the effect of the fish on the water system can be described by the following empirical chemical equation provided by a commercial fish farm:

$$\begin{aligned} 1 \text{ kg feed} + 0.45 \text{ kg } O_2 + \text{water} \longrightarrow\ & 0.9 \text{ kg fish biomass} + 0.48 \text{ kg } CO_2 \\ & + 0.047 \text{ kg } NH_3 + \text{waste} \end{aligned} \tag{3.1}$$

This assumption is based on the premise that the fish receives an adequate amount of feed. In practice, this is determined by monitoring any excess feed and the behavior of the fish. However, there may be instances where the feed is limited for a period, such as when the water is contaminated. In such situations, the biomass growth rate may decrease, and the fish may consume only what is necessary for survival. Nonetheless, in this study, we assume that the fish consumes all the provided feed and that the water quality remains within acceptable limits, thereby not affecting the fish metabolism. In reality, the apparent feed conversion ratio (which is assumed to be 0.9 $kg_{biomass}$ per kg_{feed}) reduces at higher CO_2 concentrations (Khan et al., 2018). However, this effect is not taken into account in this paper. Although the reaction coefficients may vary depending on the fish size, we assume that they are independent for simplicity. That is, we presume that they hold these values during a particular stage in the fish's life cycle while using a standard food type for Atlantic salmon. If the same

system is operated throughout a significant part of the fish's life cycle or if the food composition changes, a correction of these coefficients may be necessary.

The water treatment system is assumed to be unaffected by fish biomass. Only the consumption of oxygen, as well as the production of carbon dioxide and ammonia, are taken into account as factors that could impact the water treatment process.

The feeding rate in the fish tank typically increases exponentially over a 90-day period as the fish grows from approximately 200 g to 400 g. However, in this paper, we only focus on the first day of operation with a constant fish feed rate of 580.6 g/min.

In the biofilter, nitrifying bacteria convert ammonia to nitrite and then to nitrate, a process known as nitrification (Schreier et al., 2010). In our simulations, we assume that 97% of the TAN (total ammonia nitrogen) is converted, following the overall reaction:

$$\mathrm{NH_3} + 2\,\mathrm{O_2} \longrightarrow \mathrm{NO_3}^- + \mathrm{H}^+ + 2\,\mathrm{H_2O} \tag{3.2}$$

In addition to the biological reactions, it is assumed that all water streams in the process comply with the following acid-base equilibrium reactions:

$$\mathrm{H_2CO_3} \overset{K_1}{\rightleftharpoons} \mathrm{H}^+ + \mathrm{HCO_3}^- \tag{3.3}$$

$$\mathrm{HCO_3}^- \overset{K_2}{\rightleftharpoons} \mathrm{H}^+ + \mathrm{CO_3}^{2-} \tag{3.4}$$

$$\mathrm{NH_4}^+ \overset{K_3}{\rightleftharpoons} \mathrm{H}^+ + \mathrm{NH_3} \tag{3.5}$$

$$\mathrm{H_2O} \overset{K_w}{\rightleftharpoons} \mathrm{H}^+ + \mathrm{OH}^- \tag{3.6}$$

where K_1, K_2, K_3 and K_w are the equilibrium constants for reactions (3.3)-(3.6). The concentrations of the components in the acid-base reactions depend on pH, which in this paper is computed as

$$\mathrm{pH} = -\log_{10}(c_{H^+}/c^0) \tag{3.7}$$

where c^0=1 mol/l.

In reaction (3.3), we assume that H_2CO_3 accounts for both H_2CO_3 and dissolved CO_2, which means that the equilibrium constant, K_1, also accounts for equilibrium between these two species, represented by the following equilibrium reaction:

$$\mathrm{CO_2} + \mathrm{H_2O} \overset{K_0}{\rightleftharpoons} \mathrm{H_2CO_3} \tag{3.8}$$

Reaction (3.8) has an equilibrium constant of about $K_0 = 1.2\text{e-}03$ in water, meaning that the concentration of dissolved CO_2 is about 1000 times larger than

H_2CO_3. Nevertheless, we represent all dissolved CO_2 and H_2CO_3 as H_2CO_3 in our model.

The model's operational parameters are presented in Table 3.1, and the physicochemical parameters are listed in Table 3.2. It is important to note that the equilibrium constants used are not for pure water, but for a mixture of seawater and pure water with a salinity of 15 g/kg and temperature of 14°C. The salinity and temperature have a direct impact on the solubility of the compounds, thereby affecting the equilibrium constants. As a result, there is a shift in the equilibrium graphs compared to fresh water at 25°C (refer to Figures 3.2(a) and 3.2(b)).

Table 3.1: Operational parameters

Parameter	Value	Unit	Description
ξ^B	0.97	-	Biofilter conversion of TAN
P_{oper}	1	bar	Stripper operating pressure
f_{air}	0.3324	-	Stripper air bypass fraction
V^T	2300	m^3	Tank liquid volume
V^B	282.5	m^3	Biofilter liquid volume

Table 3.2: Physicochemical parameters at temperature of 14°C, pressure of 1 bar and salinity of 15 g/kg

Parameter	Value	Unit	Description
K_1	8.9002e-07 [a]	mol/L	Equilibrium constant of reaction (3.3)
K_2	4.3112e-10 [a]	mol/L	Equilibrium constant of reaction (3.4)
K_3	9.1592e-10 [b]	mol/L	Equilibrium constant of reaction (3.5)
K_w	5.2132e-15 [c]	mol^2/L^2	Equilibrium constant of water dissociation
K_H	5.8695e-02 [d]	mol/(L bar)	From Henry's constant for CO_2 in water
$[O_2]_{sat}$	9.39 [e]	mg/L	O_2 concentration at 100% saturation
$y^{in}_{CO_2}$	4.15e-04 [f]	-	CO_2 mole fraction in air (Sept. 2021)
M_{NH_3}	17.031	g/mol	NH_3 molar mass
M_{CO_2}	44.010	g/mol	CO_2 molar mass
$M_{NO_3^-}$	62.005	g/mol	NO_3^- molar mass
M_{O_2}	31.998	g/mol	O_2 molar mass

[a] Millero et al. (2006);
[b] Johansson and Wedborg (1980);
[c] Bandura and Lvov (2006), and Millero and Huang (2009);
[d] Weiss (1974);
[e] Benson and Krause (1984);
[f] California Institute of Technology (2021)

Three important variables for the model are TAN, TIC, and alkalinity. These may be viewed as pseudo-components, but, throughout this work, they are included in the components category for simplicity. These pseudo-components are

reaction invariants with respect to the equilibrium reactions (3.3)-(3.6), meaning that they are only affected by the in- and outflows of each unit and by the biochemical reactions (3.1) and (3.2). The TAN, TIC, and alkalinity concentrations are defined as follows:

$$c_{TAN} = c_{NH_3} + c_{NH_4^+} \tag{3.9}$$

$$c_{TIC} = c_{H_2CO_3} + c_{HCO_3^-} + c_{CO_3^{2-}} \tag{3.10}$$

$$c_{alk} = c_{OH^-} + c_{HCO_3^-} + 2c_{CO_3^{2-}} - c_{H^+} + c_{NH_3} \tag{3.11}$$

It is important to note that these concentrations are typically measured in the laboratory. There are several ways to derive these reaction invariants, and it should be noted that they are not unique since different combinations can be made. One straightforward method is to formulate atom balances for nitrogen, carbon, hydrogen, and oxygen, which involve the eight components that participate in the equilibrium reactions (3.3)-(3.6). TAN can be obtained directly from the nitrogen (N) atom balance, while TIC can be obtained directly from the carbon (C) atom balance. The alkalinity can be derived by stoichiometric considerations (Gustafsson and Waller, 1983) or by combining all four atom balances (H, O, C, N).

Assuming equilibrium in reactions (3.3)-(3.5), Figures 3.2(a) and 3.2(b) illustrate the mole fractions for the carbonate system and ammonia system relative to TIC and TAN as a function of pH, respectively. To maintain low levels of both H_2CO_3 and NH_3 in the fish tank, the pH should be kept within a specific range. From the figures, it is apparent that a pH level above 7 is desirable to achieve low concentrations of H_2CO_3, whereas a pH level below 8 is necessary to achieve low concentrations of NH_3. Thus, a pH range between 7 and 8 is optimal for the fish tank.

The nitrifying bacteria in the biofilter are adaptable to pH, but they do not function well at pH levels below 6 or above 10. The optimal range for their activity is between 7.5 and 8, as reported by Raoeliaritiana (2016). Therefore, it is assumed that a satisfactory conversion range falls between 7 and 8. To increase the efficiency of the stripper, it is desirable to have high concentrations of CO_2 (or H_2CO_3 equivalent), as depicted in Figure 3.2(a). This requires a low pH level to achieve high levels of TIC in the form of H_2CO_3. In practice, it may be better to operate the biofilter at a pH of around 7 to achieve optimal stripper efficiency, although a higher pH level would be better for the bacteria's activity. Alternatively, adding acid between the biofilter and the stripper could resolve this conflict, but this approach is not explored in this study.

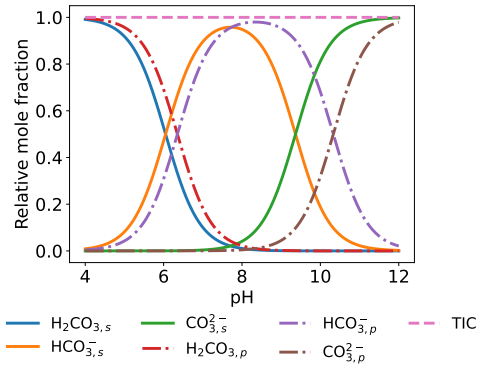

(a) Carbonate system (TIC)

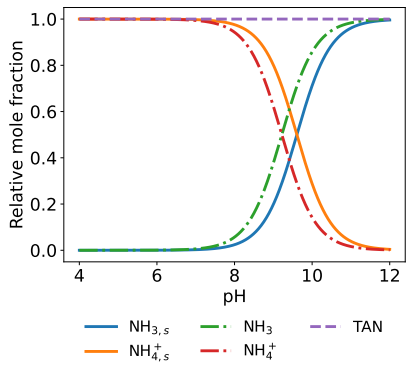

(b) Ammonia-ammonium system (TAN)

Figure 3.2: Relative mole fraction for **(a)** carbonate system (TIC) and **(b)** ammonia system (TAN) as a function of pH. Subscript s (solid lines) are values computed for salinity 15 g/kg at temperature 14°C, and subscript p are values computed for pure water at 25°C.

3.4 Process Model

3.4.1 Model assumptions

For simplicity, this section describes all assumptions and the steady-state molar balances, which are then extended to the dynamic model.

The main assumption made for the model is that the system can be described by the chemical reactions (3.1)-(3.6). Additionally, several assumptions were made, including:

1. All food is consumed by the fish and the conversion is defined by reaction (3.1). The biomass increases the mass of the fish, but it is assumed that it does not affect the stoichiometry of reaction (3.1).

2. The tank and the biofilter are modeled as continuous stirred-tank reactors.

3. Nitrification is assumed to occur only in the biofilter with operating conditions to achieve a given efficiency of TAN conversion according to reaction (3.2).

4. The stripper is modeled as an equilibrium-stage column with a given air bypass to represent that the real column has less than one equilibrium stage while neglecting the holdup.

5. Neither carbon dioxide nor oxygen is lost to the air in the fish tank or biofilter. Additionally, the variation of the oxygen concentration in the stripper is neglected.

6. The makeup water does not contain TIC, TAN, or alkalinity and does not affect the salinity of the system.

7. Temperature is assumed to be perfectly controlled and to not affect fish metabolism or vice versa.

8. The only relevant addition of water is the makeup water and the only relevant removal is the purge.

9. The levels of the tank and the biofilter are considered perfectly controlled.

These assumptions provide a simplified model for the system, and although they may not capture all the complexities of the real system, they allow for a reasonable estimation of the system's behavior.

The two main approaches for modelling the stripping column are the equilibrium-stage model and the two-film mass transfer model. In Vinci et al. (1996), the authors provided a detailed analysis of the latter, which may be more realistic than an equilibrium model. However, this model involves equations with decimal exponents, which can generate imaginary numbers when facing negative arguments during the root-finding process. Therefore, we decided to use an equilibrium-stage model with one stage and a bypass, as in Assumption 4, due to its simplicity and fewer numerical issues. The bypass introduces some non-ideality, which may be realistic since some air volumes may pass through the stripper without reaching equilibrium with the water. Figure 3.3 illustrates this modelling approach.

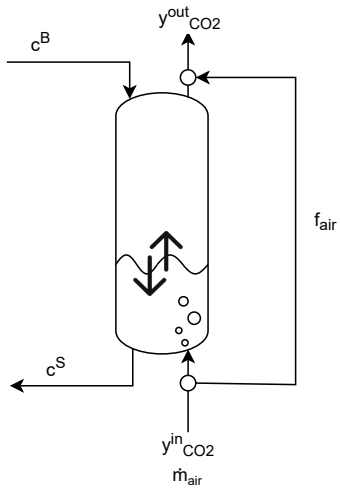

Figure 3.3: Simplified model representation of stripper with single equilibrium stage and partial bypass of air.

The bypass fraction was determined by comparing the model results with those from an experimental packed column. The column was operated with an inlet CO_2 concentration of 20 mg/L (0.45 mmol/L) and a volumetric gas-to-liquid ratio of 5 and was found to remove 60% of the CO_2 (Summerfelt et al., 2000). Based on this data, the calculated bypass fraction was determined to be 33.24% of the air inlet, as shown in Table 3.1. It should be noted that as per Assumption 4, the stripper holdup is neglected in the model, resulting in a static stripper model.

3.4.2 Steady-state molar balances

Based on the aforementioned assumptions, we present below the steady-state molar balances for water, alkalinity, TIC, TAN, nitrate, and oxygen. The variables' names and units are:

- Molar concentration, c [mol/m^3_{water}]=[mmol/L_{water}]
- Mass concentration, w [mg/L_{water}]
- Liquid flow rate, q [m^3_{water}/min]
- Molar flow rate, $\dot{m}$ [mol/min]

3.4.2.1 Molar balances for water

When considering the mass balance for the mixing point of makeup water, the independent variables or degrees of freedom are the makeup water flow rate, denoted as q^m, and the recirculation flow rate, denoted as q. Based on this, the following equation is obtained:

$$q^B = q + q^m \tag{3.12}$$

It is assumed that the liquid holdups remain constant at all times. Therefore, the purge flow is equal to the makeup flow (q^m), and the liquid flow rate is q after the purge and before the makeup points. After the makeup and before the purge, the liquid flow rate is q^B, as illustrated in Figure 3.1.

3.4.2.2 Molar balances for alkalinity

- Tank:

$$qc^T_{alk} = qc^{in}_{alk} + \dot{m}^T_{buffer} + \dot{m}^T_{base} + \lambda_{NH_3} F \tag{3.13}$$

where $\dot{m}^T_{buffer}$ and $\dot{m}^T_{base}$ are the molar flow rates of $NaHCO_3$ (HCO_3^-) and NaOH (OH^-), respectively, being added in the tank. F is the fish feed rate,

and λ_{NH_3} is the stoichiometric coefficient for NH_3 in the fish metabolism (reaction 3.1), given by:

$$\lambda_{NH_3} = \frac{0.047}{M_{NH_3}} {}^{mol}/_{g_{feed}}$$

where M_{NH_3} is the molar mass of NH_3.

- Biofilter:

$$q^B c^B_{alk} = q c^T_{alk} + \dot{m}^B_{buffer} + \dot{m}^B_{base} - 2\xi^B q c^T_{TAN} \tag{3.14}$$

where $\dot{m}^B_{buffer}$ and $\dot{m}^B_{base}$ are the molar flow rates [mol/min] of $NaHCO_3$ and NaOH, respectively, being added in the biofilter. The last term $-2\xi^B q c^T_{TAN}$ comes from reaction (3.2), in which alkalinity has a stochiometric coefficient of -2 because it forms H^+ and consumes NH_3.

- Stripper:

$$c^S_{alk} = c^B_{alk} \tag{3.15}$$

3.4.2.3 Molar balances for total inorganic carbon (TIC)

- Tank:

$$q c^T_{TIC} = q c^{in}_{TIC} + \dot{m}^T_{buffer} + \lambda_{CO_2} F \tag{3.16}$$

where $\dot{m}^T_{buffer}$ is the molar flow rate of $NaHCO_3$ being added in the tank, λ_{CO_2} is the stoichiometric coefficient for CO_2 in the fish metabolism (reaction 3.1), which is given by

$$\lambda_{CO_2} = \frac{0.48}{M_{CO_2}} {}^{mol}/_{g_{feed}}$$

- Biofilter:

$$q^B c^B_{TIC} = q c^T_{TIC} + \dot{m}^B_{buffer} \tag{3.17}$$

where $\dot{m}^B_{buffer}$ is the molar flow rate of $NaHCO_3$ being added in the biofilter.

- Stripper: Assume CO_2 equilibrium between gas and liquid outflow and use the bypass fraction f_{air} to represent that the real stripper has less than one

equilibrium stage.

$$q^B c^S_{TIC} + (1 - f_{air})\dot{m}^I_{air} \frac{y^{out}_{CO_2}}{1 - y^{out}_{CO_2}} = q^B c^B_{TIC} + (1 - f_{air})\dot{m}^I_{air} \frac{y^{in}_{CO_2}}{1 - y^{in}_{CO_2}} \tag{3.18}$$

$$y^{out}_{CO_2} = \frac{c^S_{H_2CO_3}}{K_H P_{oper}} \tag{3.19}$$

where $\dot{m}^I_{air}$ is the molar flow rate of air excluding its CO_2 content, and $y^{out}_{CO_2}$ is the molar fraction of CO_2 at the outlet stream, meaning that the total air flow rate at the inlet stream is given by $\dot{m}_{air} = \frac{\dot{m}^I_{air}}{1 - y^{out}_{CO_2}}$.

3.4.2.4 Molar balances for total ammonia nitrogen (TAN)

- Tank:

$$q c^T_{TAN} = q c^{in}_{TAN} + \lambda_{NH_3} F \tag{3.20}$$

- Biofilter:

$$q^B c^B_{TAN} = q c^T_{TAN} - \xi^B q c^T_{TAN} \tag{3.21}$$

- Stripper:

$$c^S_{TAN} = c^B_{TAN} \tag{3.22}$$

3.4.2.5 Molar balances for nitrate

The NO_3^- ions are only produced in the biofilter and removed by the purge, so we have at steady state:

- Tank:

$$c^T_{NO_3^-} = c^{in}_{NO_3^-} \tag{3.23}$$

- Biofilter:

$$q^B c^B_{NO_3^-} = q c^T_{NO_3^-} + \xi^B q c^T_{TAN} \tag{3.24}$$

- Stripper:

$$c^S_{NO_3^-} = c^B_{NO_3^-} \tag{3.25}$$

3.4.2.6 Molar balances for oxygen

- Tank:

$$qc_{O_2}^T = qc_{O_2}^{in} - \lambda_{O_2} F \tag{3.26}$$

where λ_{O_2} is the stoichiometric coefficient of O_2 in the fish metabolism, which is given by

$$\lambda_{O_2} = \frac{0.45}{M_{O_2}} {}^{mol}/_{g_{feed}}$$

- Biofilter:

$$q^B c_{O2}^B = qc_{O_2}^T - 2\xi^B qc_{TAN}^T \tag{3.27}$$

- Stripper:

$$c_{O_2}^S = c_{O_2}^B \tag{3.28}$$

- Purge + Oxygen cone:

$$qc_{O_2}^{in} = qc_{O_2}^S + \dot{m}_{O_2} \tag{3.29}$$

where $\dot{m}_{O_2}$ is the molar flow rate of oxygen being injected into the stream in the oxygen cone.

Note that, except for O_2, which is added between the stripper and the tank, we have that $c^{in} = c^S$.

The pH values at the different locations are calculated based on the provided concentrations of alkalinity, TIC, and TAN using Eq. (3.30), as explained next. The concentrations of ionic species can be determined from the calculated pH values using the equilibrium reactions (3.3)-(3.6).

3.4.3 Computation of pH

In addition to the molar balances of reaction invariants, the acid-base equilibrium in the system must also be considered in order to compute the pH, along with the concentration of the species in equilibrium. This was done by writing the equilibrium relations between species, according to reactions (3.3)-(3.6), and solving the resulting system of algebraic equations as a function of the reaction invariants.

A simple analytic expression for alkalinity was developed by Henson and Seborg (1994), which enables the calculation of c_{H^+} as a function of c_{TIC} and c_{alk}. We extend this analysis by including the dependence on c_{TAN} to incorporate the ammonia-ammonium equilibrium. The resulting analytic expression, which

is used to compute c_{H^+} (or pH) at each unit (fish tank, biofilter, and stripper), becomes:

$$c^i_{alk} = c^i_{TIC}\frac{K_1 c^i_{H^+} + 2K_1K_2}{(c^i_{H^+})^2 + K_1 c^i_{H^+} + K_1K_2} + \frac{K_w}{c^i_{H^+}} - c^i_{H^+} + c^i_{TAN}\frac{K_3}{c^i_{H^+} + K_3}, \quad i = T, B, S \tag{3.30}$$

In Appendix, we show in detail how this expression was derived and its extension to include the equilibrium of phosphate ions, if these are present.

3.4.4 Dynamic molar balances

This section describes the generalized model which can be utilized for simulating steady-state and dynamic behavior. The model equations are consistent with the previous sections but presented in a more general form. The model considers five species or components, namely alkalinity, TIC, TAN, NO_3^-, and O_2. The molar balances for these five components in the tank and the biofilter are described by Eq. (3.31) and (3.32), respectively.

$$V^T\frac{d\boldsymbol{c}^T}{dt} = q(\boldsymbol{c}^{in} - \boldsymbol{c}^T) + \boldsymbol{g}^T + \boldsymbol{h}^T \tag{3.31}$$

$$V^B\frac{d\boldsymbol{c}^B}{dt} = q^B\left(\boldsymbol{c}^T\frac{q}{q^B} - \boldsymbol{c}^B\right) + \boldsymbol{g}^B + \boldsymbol{h}^B \tag{3.32}$$

where $\boldsymbol{c}^{in}$, $\boldsymbol{c}^T$, $\boldsymbol{c}^B$ and $\boldsymbol{c}^S$ are column vectors containing the concentration of the five species at the inlet of the tank, in the fish tank, in the biofilter, and in the stripper, respectively. $\boldsymbol{g}^T$ and $\boldsymbol{g}^B$ are column vectors representing the amount of each component coming from input streams to the tank and biofilter, respectively, and $\boldsymbol{h}^T$ and $\boldsymbol{h}^B$ are column vectors containing the amount of each component generated or removed in the reactions (3.1) and (3.2), respectively. From this, $\boldsymbol{g}^T$, $\boldsymbol{g}^B$, $\boldsymbol{h}^T$ and $\boldsymbol{h}^B$ are defined as follows:

$$\boldsymbol{g}^T = \begin{bmatrix} \dot{m}^T_{buffer} + \dot{m}^T_{base} \\ \dot{m}^T_{buffer} \\ 0 \\ 0 \\ 0 \end{bmatrix} \qquad \boldsymbol{g}^B = \begin{bmatrix} \dot{m}^B_{buffer} + \dot{m}^B_{base} \\ \dot{m}^B_{buffer} \\ 0 \\ 0 \\ 0 \end{bmatrix}$$

$$\boldsymbol{h}^T = \begin{bmatrix} \lambda_{NH_3} F \\ \lambda_{CO_2} F \\ \lambda_{NH_3} F \\ 0 \\ -\lambda_{O_2} F \end{bmatrix} \qquad \boldsymbol{h}^B = \begin{bmatrix} -2q\xi^B c^T_{TAN} \\ 0 \\ -q\xi^B c^T_{TAN} \\ q\xi^B c^T_{TAN} \\ -2q\xi^B c^T_{TAN} \end{bmatrix}$$

The set of ordinary differential equations (ODEs) presented above comprises a total of 10 equations, which govern the dynamics of the system. In addition, there are 4 static equations that describe the molar balances in the stripper and oxygen cone.

To implement this system, we use a set of 10 differential states, as given in Eqs. (3.31) and (3.32), which are derived from the molar balances of TIC, TAN, alkalinity, oxygen, and nitrate in the tank and biofilter. We also use 4 algebraic states, as given in Eqs. (3.18) and (3.30), which calculate the values of c^S_{TIC} and c_{H^+} after passing through the three units (tank, biofilter, and stripper). Although c_{H^+} (pH) is not necessary for dynamic simulation of the tank and biofilter, unless one wants to know the pH and individual species concentrations, it is required for modelling the stripper, as the H_2CO_3 concentration is the driving force for TIC removal.

3.5 Degrees of Freedom for operation

The system can be operated through several manipulated variables (i.e., dynamic degrees of freedom), as illustrated in Figure 3.4. These variables are:

1. Fish feed (pellets);
2. Recirculation flow (i.e., liquid inflow to tank);
3. Liquid outflow from the tank;
4. Liquid inflow to biofilter;
5. Liquid outflow from biofilter;
6. Liquid outflow from stripper:

7. Liquid inflow to oxygen unit;
8. Pure oxygen feed;
9. Heating/cooling;
10. Purge;
11. Makeup water;
12. Air inflow to stripper;
13. Base/buffer added to tank/biofilter

The last variable could potentially represent up to four degrees of freedom, although typically only one is used at a time. When proposing the model, it was assumed constant liquid holdup in the fish tank, biofilter, stripper, oxygen unit, mixing point for makeup water, and exit point for purge. This enabled us to establish six molar balances, which we could utilize to eliminate six of the previously mentioned variables. For instance, by taking into account the total holdup in all units, we determined that the purge flow was equal to the makeup water flow rate, q^m. Additionally, the feed to the biofilter was equivalent to the sum of the liquid flow out of the fish tank and the makeup water. Furthermore, the liquid flow rate of the outlet of the fish tank, biofilter, stripper, and oxygen unit was equivalent to their respective inlet flow rates. To simplify the system further, we assumed that the temperature of the liquid streams was perfectly controlled, removing the heating/cooling as a degree of freedom. In total, this eliminates seven degrees of freedom, leaving us with six steady-state degrees of freedom for operation and control. For our simulations, we consider the fish feed, F, as a measured disturbance. As a result, we focus on the five degrees of freedom (manipulated variables) for operation, which are provided in Table 3.3.

Table 3.3: Control degrees of freedom (manipulated variables) with steady-state effect

Description	Variable	Unit
Recirculation flow rate	q	$\mathrm{m}^3/\mathrm{min}$
Air feed to stripper	$\dot{m}_{air}$	$\mathrm{mol}/\mathrm{min}$
Oxygen feed	$\dot{m}_{O_2}$	$\mathrm{mol}/\mathrm{min}$
Makeup water	q^m	$\mathrm{m}^3/\mathrm{min}$
Base/buffer feed	$\dot{m}_{base}/\dot{m}_{buffer}$	$\mathrm{mol}/\mathrm{min}$

The process flowsheet is shown in Figure 3.4, with the first four degrees of freedom indicated with valve symbols. The degree(s) of freedom related

to buffer/base addition is not assigned in this flowsheet, as it can be any of the buffer/base feed streams. Moreover, the flowsheet includes two stabilizing controllers to control the nitrate and oxygen concentrations in the tank, which are later used in the dynamic simulations.

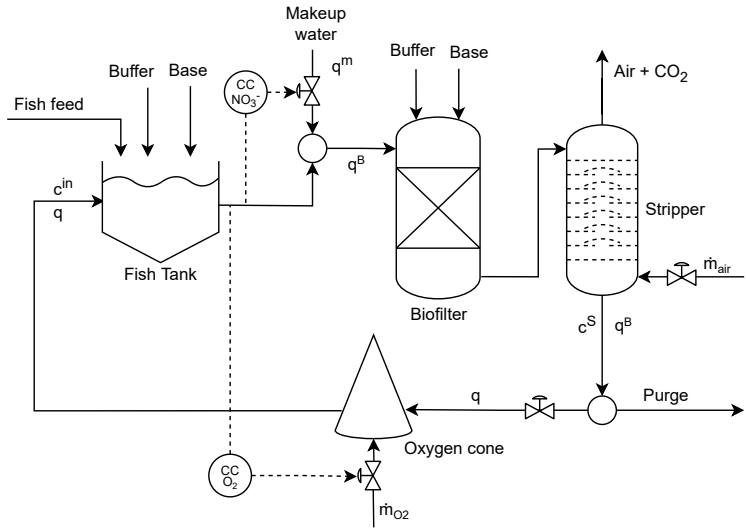

Figure 3.4: Flowsheet of RAS process where the valve symbols show control degrees of freedom. Two stabilizing controllers for nitrate and oxygen are included. In addition, we usually have a stabilizing pH controller using buffer/base addition.

With a given feed rate, there are five steady-state operational degrees of freedom, and therefore we need five specifications to define the operation. In the simulations, we use a typical set of specifications provided in Table 3.4. Out of these specifications, two are on manipulated variables (MVs), namely the recirculation flow rate and air feed to the stripper, while the other three are on controlled variables (CVs). These three CV specifications (O_2 saturation, nitrate concentration, and pH) indirectly determine the value of the three remaining MVs (O_2 feed, makeup water, base/buffer addition).

Table 3.4: Nominal operational specifications used in simulations

Variable	Value	Unit	Description
q	30	$\mathrm{m}^3/\mathrm{min}$	Recirculation flow rate
$\dot{m}_{air}$	6285	$\mathrm{mol}/\mathrm{min}$	Air feed to stripper
$c_{O_2\%}$	80%	-	O_2 saturation
$w^T_{NO_3^-}$	100	mg/L	NO_3^- mass concentration in fish tank
pH^B	7.05	-	pH in biofilter
F	580.6	g/min	Fish feed rate on day 1

3.6 Simulation results

In this section, we present some steady-state and dynamic simulation results, which also contribute to validating the model.

3.6.1 Steady-state simulations

For the steady-state calculations, we utilized the five specifications in Table 3.4 in combination with the given feed rate. It is worth noting that we maintained the oxygen level, the nitrate level, and the pH in the biofilter at fixed values. To achieve control of the pH in the biofilter, we considered four different scenarios, where we implemented one type of pH/alkalinity adjustment at a time (see Figure 3.4):

Scenario 1) Base addition in the tank ($\dot{m}^T_{base}$)

Scenario 2) Base addition in the biofilter ($\dot{m}^B_{base}$)

Scenario 3) Buffer addition in the tank ($\dot{m}^T_{buffer}$)

Scenario 4) Buffer addition in the biofilter ($\dot{m}^B_{buffer}$)

The steady-state system was solved for the four scenarios considering the conditions for day 1. The makeup water flow rate was the same in all scenarios ($q^m = 0.992$ $\mathrm{m}^3/\mathrm{min}$) because the nitrate concentration was specified. Since the recirculation flow rate, q, was specified at 30 $\mathrm{m}^3/\mathrm{min}$, the recirculation ratio was $r = q/(q + q^m) = 0.968$ in all scenarios. The oxygen feed rate was constant for all scenarios at 11.49 $\mathrm{mol}/\mathrm{min}$. The results presented in Table 3.5 indicate that the amount of base or buffer is the same regardless of the location where it is added.

Table 3.5: Required addition of **base** (NaOH) or **buffer** (NaHCO3) to keep desired pH in biofilter in each scenario [mol/min]

Variable	Scenario 1	Scenario 2	Scenario 3	Scenario 4
$\dot{m}^T_{base}$	3.75	0	0	0
$\dot{m}^B_{base}$	0	3.75	0	0
$\dot{m}^T_{buffer}$	0	0	5.46	0
$\dot{m}^B_{buffer}$	0	0	0	5.46

Tables 3.6-3.9 present the results obtained from the steady-state simulation. We see that the pH in the fish tank was generally higher than in the biofilter in most scenarios, except in Scenario 2 where base was added to the biofilter. The decrease in TAN and oxygen concentrations from the tank to the biofilter can be attributed to reaction (3.2) and dilution by the makeup water. In terms of maximizing fish growth, low levels of NH_3 and CO_2 (H_2CO_3) are preferred in the fish tank. The pH in the fish tank significantly affects these values. For instance, a high pH of 7.33 resulted in a high concentration of ammonia (Scenario 1), while a low pH of 7.02 resulted in a high concentration of H_2CO_3 (Scenario 2). To achieve low levels of CO_2, it is better to use NaOH (base) (Scenarios 1 and 2) instead of $NaHCO_3$ (buffer) for pH adjustment.

Despite using a large amount of buffer, Scenarios 3 and 4, which both use sodium bicarbonate (buffer) for pH adjustment, have almost identical steady-state values. This result is expected due to the well-known buffer effect.

Table 3.6: Steady-state concentrations [mmol/L or -] for each unit for Scenario 1

Variables	Tank	Biofilter	Stripper
c_{alk}	2.26	2.07	2.07
c_{TIC}	2.34	2.27	2.13
$c_{H_2CO_3}$	0.12	0.21	0.08
c_{TAN}	0.055	0.0016	0.0016
c_{NH_3}	2.89e-04	4.42e-06	1.07e-05
$c_{NO_3^-}$	1.61	1.61	1.61
c_{O_2}	0.23	0.12	0.12
pH	7.33	7.05	7.44

Table 3.7: Steady-state concentrations [mmol/L or -] for each unit for Scenario 2

Variables	Tank	Biofilter	Stripper
c_{alk}	2.12	2.07	2.07
c_{TIC}	2.34	2.27	2.13
$c_{H_2CO_3}$	0.23	0.21	0.08
c_{TAN}	0.055	0.0016	0.0016
c_{NH_3}	1.42e-04	4.42e-06	1.07e-05
$c_{NO_3^-}$	1.61	1.61	1.61
c_{O_2}	0.23	0.12	0.12
pH	7.0186	7.05	7.44

Table 3.8: Steady-state concentrations [mmol/L or -] for each unit for Scenario 3

Variables	Tank	Biofilter	Stripper
c_{alk}	3.85	3.62	3.62
c_{TIC}	4.09	3.96	3.71
$c_{H_2CO_3}$	0.27	0.36	0.13
c_{TAN}	0.055	0.0016	0.0016
c_{NH_3}	2.12e-04	4.42e-06	1.16e-05
$c_{NO_3^-}$	1.61	1.61	1.61
c_{O_2}	0.23	0.12	0.12
pH	7.2	7.05	7.47

Table 3.9: Steady-state concentrations [mmol/L or -] for each unit for Scenario 4

Variables	Tank	Biofilter	Stripper
c_{alk}	3.67	3.62	3.62
c_{TIC}	3.92	3.96	3.71
$c_{H_2CO_3}$	0.27	0.36	0.13
c_{TAN}	0.055	0.0016	0.0016
c_{NH_3}	2.04e-04	4.42e-06	1.16e-05
$c_{NO_3^-}$	1.61	1.61	1.61
c_{O_2}	0.23	0.12	0.12
pH	7.18	7.05	7.47

3.6.2 Dynamic simulation

Figure 3.5 illustrates the dynamic response of the system to a step increase of 56.5 g/min in the fish feed (about 10% disturbance) with all the five manipulated

variables kept constant, including the oxygen addition.

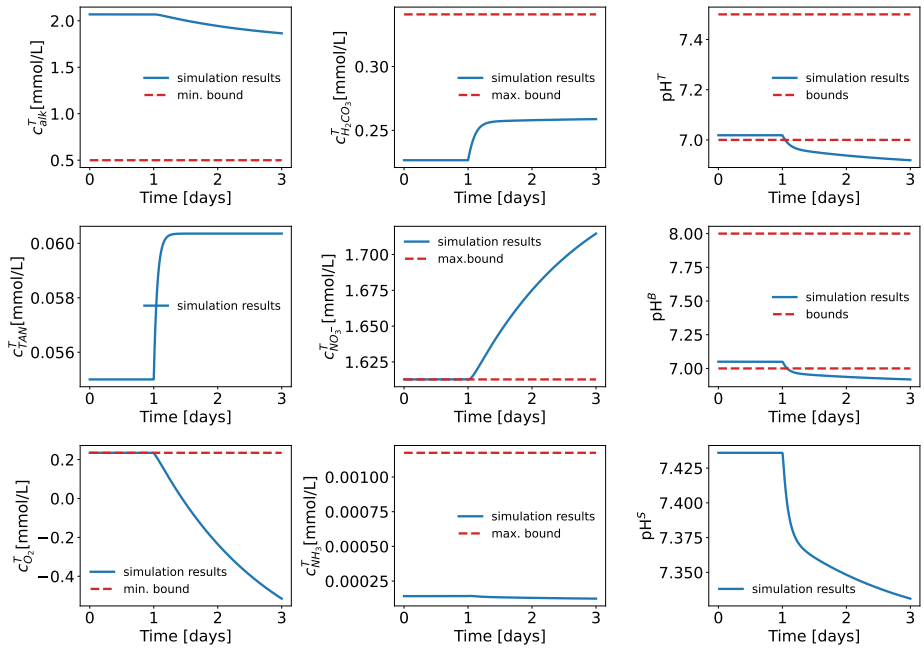

Figure 3.5: Dynamic behavior for a step change of 56.5 g/min in the fish feed, F, at day 1, with no oxygen and nitrate control.

The simulation results indicated that the fish would not survive, even for a day, mainly due to the oxygen level becoming negative in less than one day. This result was caused by the consumption of oxygen according to reaction (3.1). Furthermore, the nitrate concentration steadily increased, which is harmful to the fish.

To prevent negative oxygen levels and the buildup of nitrate in the system, the oxygen intake was controlled in the fish tank, and makeup water addition was used to control nitrate in the tank, as shown in Figure 3.4.

With those controllers, we see in Figure 3.6 that oxygen and nitrate concentrations are now kept constant, but other variables still go out of bounds, including the pH in the tank and in the biofilter. This indicates the need to introduce additional control loops, using buffer or base addition. However, since the aim of this work was to present the process modeling, a more detailed control design will be considered in future work.

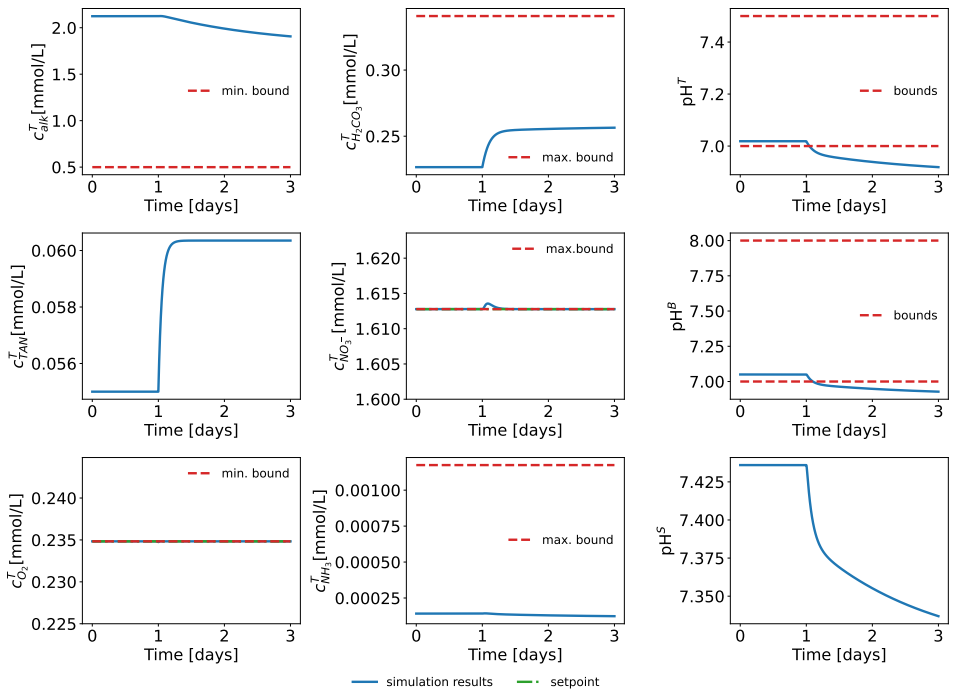

Figure 3.6: Dynamic behavior for a step change of 56.5 g/min in the fish feed, F, at day 1, with oxygen and nitrate controllers.

3.7 Comparison with real data

To validate the model, we compared it to data collected from a commercial fish farm of Atlantic salmon that used the same RAS configuration as in Scenario 2, where base was added to the biofilter to regulate the pH. The data was collected over a 44-day period and consisted of sensor readings taken every 30 minutes, including temperature (T), salinity (S), oxygen saturation ($c_{O_2\%}$), and pH in the fish tank (pH^T) and stripper (pH^S), as well as various flow rates. Laboratory measurements were also taken every other day on the outflow from the tank, which included the concentrations of NO_3^-, H_2CO_3, TAN, and alkalinity (c_{alk}). Figure 3.7 displays the average daily measurements of temperature and salinity.

In Figure 3.8, we compare the measured data with the simulated dynamic responses. The upper six plots display the six operational degrees of freedom, including the fish feed. The lower nine plots show six concentrations in the fish tank (T) along with the pH after the fish tank, biofilter, and stripper.

The simulation model is similar to the one described earlier, with the exception of the stoichiometric coefficient for ammonia in reaction (3.1), which was halved

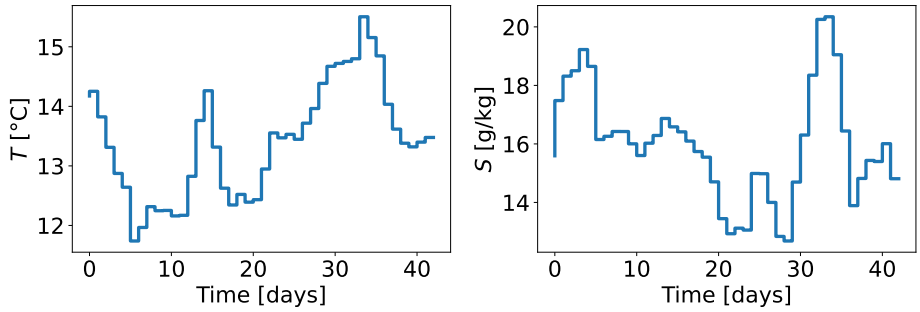

Figure 3.7: Temperature and salinity measured data.

to 0.0235 to better match the experimental data for TAN concentration in the fish tank. The variation in the stoichiometric coefficients is expected as they depend on the composition of the fish feed. Since the measured temperature and salinity are not constant, the equilibrium constants change slightly over time as they are a function of temperature and salinity.

It is important to note that the simulated responses were not generated by directly entering the independent variables, *i.e.*, feed flow rates, into the dynamic model. This is because some flow rates were missing from the data, such as air and oxygen inlet streams, and directly entering the measured base flow rate would have resulted in significant offsets in pH and other concentrations. This is due to the model predictions being highly sensitive to errors in the base feed flow rate. Instead, the pH and concentration measurements were used as setpoints, since these are more reliable, and feedback controllers were employed to adjust the feed flow rates and match them with the measured values.

In order to match the simulation results with the measured data, several adjustments were made to the model inputs. The details of these adjustments are outlined below:

- The measured data for fish feed, denoted as F, was used in the model after excluding the very small values. To account for situations where the fish stop eating and operators stop feeding (which leads to these excluded values), the feed rate was always set to be higher than a minimum amount of $50\%F^i$, where F^i is the planned amount of feed for day i. Moreover, due to the nature of the data, which reports the cumulative mass of food each day, we assumed a step-like feed rate for each day, which may result in occasional large deviations in concentrations.

- The measured rate of makeup water, q^m, was used directly in the model.

- The measured recirculation rate, q, was also used directly in the model. It remained almost constant over the 44-day period, except for two days with slightly lower values.
- The airflow to the stripper, $\dot{V}_{air}$, was not measured, so it was assumed to be 10 times the recirculation flow rate of project, which was assumed to be 23.7 m^3/min (the mean of all q).
- The flow rate of the oxygen inlet was not measured. It was estimated by matching the measured and simulated oxygen concentrations using a feedback O_2 controller with the measured oxygen saturation as the setpoint.
- The base addition was calculated by matching the measured and simulated pH after the stripper, using a feedback pH controller with the daily average of measured pH as the setpoint. To improve the match with other measured data, such as alkalinity and CO_2/H_2CO_3 concentrations in the fish tank, a bias of 0.2 pH units was introduced for the measured pH after the stripper. This means that the simulated pH after the stripper is 0.2 units lower than the measured value (see the lower right plot in Figure 3.8).

The calculated base addition showed significant deviations from the measured value, particularly during the first 14 days, which could be attributed to measurement errors. The later deviations or peaks could be explained by inaccuracies in the feed rate F, leading to errors in the CO_2 produced by fish metabolism, and thereby affecting the pH and the amount of base required. The bias of 0.2 pH units introduced in the stripper was carried over to the fish tank, resulting in a similar deviation. The reason for the deviation could be a sensor error or modelling inaccuracies in the thermodynamics, which were not modelled in much detail. The simulated concentrations of TAN, alkalinity, and H_2CO_3 in the fish tank were in good agreement with the measured values from the laboratory. The simulated pH was also close to the measured values, except for the bias of about 0.2 pH units.

In Assumption 3, the constant conversion of TAN might not always reflect reality. The operating region under study includes a change in behavior of the conversion of TAN, where a constant value provides a better representation of reality (0.1 to 0.5 mg_{TAN}/L), and beyond which the Monod model might be more suitable (when TAN mass concentration exceeds 0.5 mg/L) (Malone et al., 2006). To evaluate the impact of TAN conversion on concentrations, a sensitivity analysis was conducted, revealing that it only had a significant effect on TAN concentration. This can be attributed to the disparity in magnitudes between nitrate and ammonia quantities, resulting in the efficiency effect being negligible on nitrate concentration. Consequently, the nitrate concentration is primarily

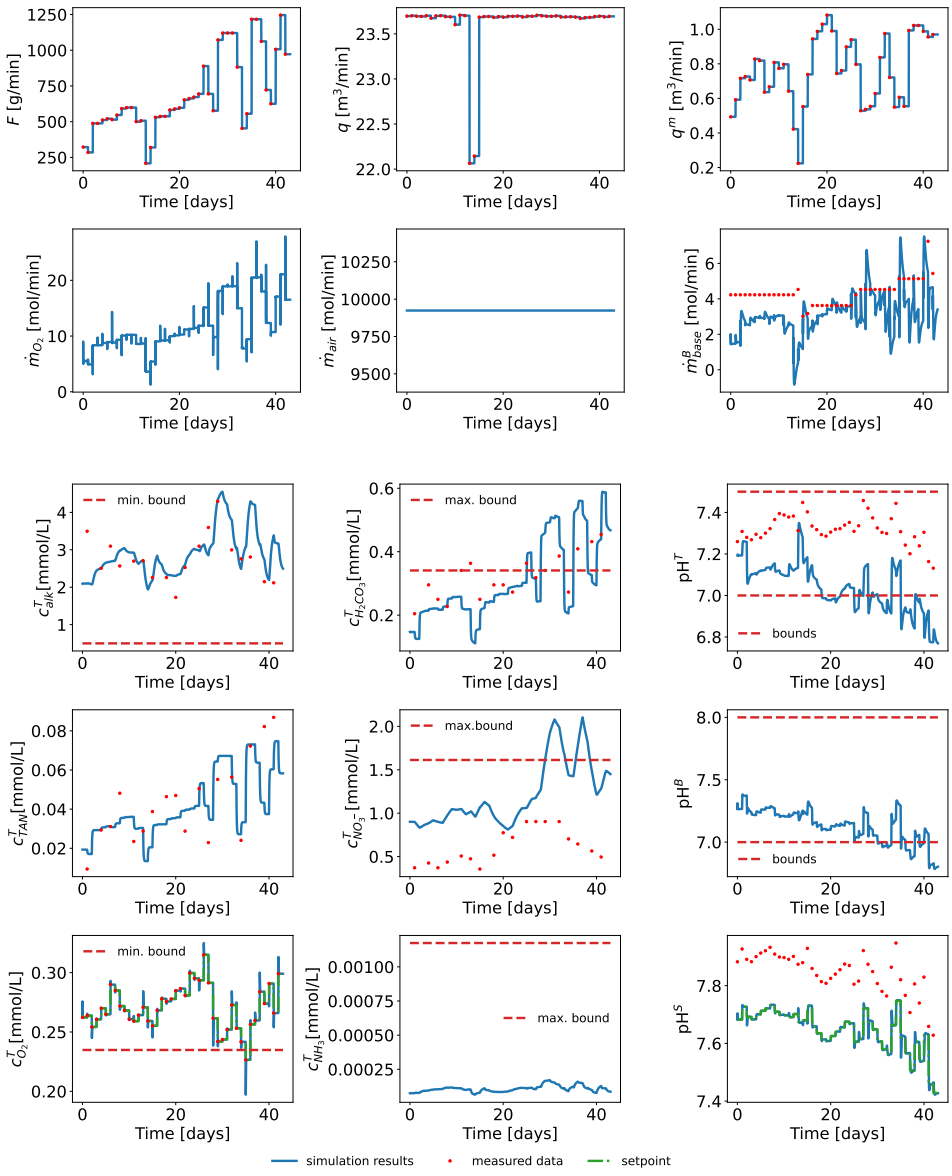

Figure 3.8: Simulated (blue lines) and measured (red dots) flow rates and concentrations for a real RAS plant over a 44-day period.

influenced by purge/makeup water. Figure 3.9 illustrates that the amount of nitrate formation in the biofilter is insufficient to significantly impact its concentration.

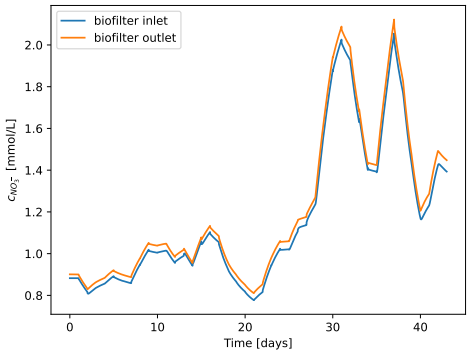

Figure 3.9: Nitrate concentrations before and after the nitrification in the biofilter.

The simulated nitrate concentration was approximately twice the measured value, which could be attributed to the accumulation of nitrate in the recirculating system due to the small purge. In the model, some of the nitrogen from the feed exits the system in the purge, mainly as nitrate. Since the simulated TAN concentration in the fish tank was similar to the measured values, it is likely that the actual system has other nitrate exits, such as in solid waste and denitrification in the biofilm. However, the model did not account for solids or denitrification. Therefore, the fish farm system could benefit from nitrate control to better use of the makeup water.

3.8 Discussion

3.8.1 Stripper model

At first, we attempted to model the stripper by assuming a constant efficiency. However, this resulted in the existence of multiple solutions, each of them in a different pH zone. Therefore, it was numerically better and more physically correct to model the stripping unit as a single-stage equilibrium column with some air bypass. In this model, the efficiency was indirectly dependent on the pH, as the concentration of H_2CO_3 available for stripping depends on pH.

3.8.2 Numerical solver

CasADi is an open-source tool that enables nonlinear optimization and algorithmic differentiation. Its symbolic framework facilitates model simulation

and implementation of numerical optimal control, which is the intended focus of future work. The equation systems were solved using CasADi version 3.5.5 in Python version 3.8.8, and required a DAE solver, so IDAS from SUite of Nonlinear and DIfferential/ALgebraic equation Solvers (SUNDIALS) (Hindmarsh et al., 2005), distributed along with CasADi, was used for the steady-state and dynamic simulations.

3.8.3 Use of reaction invariants

In this work, the model development relied on incorporating three reaction invariants, namely TAN, TIC, and alkalinity. Instead of representing individual components, including pH, as dynamic states, static equilibrium relationships like Eq. (3.30) were used to obtain their concentrations.

An alternative, and more straightforward, approach for this modelling involves writing dynamic balances for all chemical components and introducing four extents of reactions to represent reactions (3.3)-(3.6). This model was also implemented, and the results agree with the model presented in this work, which serves as validation of the proposed model. While the model based on the extent of reactions avoids the use of reaction invariants, which can be non-physical quantities, it results in numerical difficulties. The steady-state solution was highly dependent on the initial condition, often leading to infeasibility with negative concentrations. To overcome this issue, a numerical trick was used by making these states equal to the exponential of the concentrations. While this solved the infeasibility problem, the numerical solver could still diverge with the iterations approaching very high concentrations. Thus, the approach based on reaction invariants was preferred as it was more stable and reliable.

3.8.4 Steady-state simulations

The steady-state simulation yielded valuable insights into the system. Because of the nitrate requirement, the amount of makeup water was constant in all scenarios. To decrease the amount of the makeup water, one may add a denitrification unit to the process to convert nitrate into nitrogen gas, as suggested by Tal et al. (2009).

The steady-state results presented in Tables 3.6-3.9 indicate that the concentration of H_2CO_3 in the tank was the lowest in Scenario 1 ($c^T_{H_2CO_3} = 0.13$ mmol/L), where base was added in the biofilter, which is preferable for fish growth since they thrive best with low H_2CO_3 levels (Khan et al., 2018). On the other hand, the pH in the tank was also the highest in Scenario 1 (pH^T = 7.33), resulting in a high concentration of ammonia ($c^T_{NH_3} = 2.89$ e-04 mmol/L). Previous research has shown that high H_2CO_3 levels have a negative impact on

fish growth, while high ammonia concentrations induce stress, which also affects growth (Thorarensen and Farrell, 2011).

3.9 Conclusion

The generalized and simplified steady-state and dynamic models of a Recirculating Aquaculture System (RAS) water treatment were developed for control and optimization purposes.

Dynamic simulation of a nominal case with no control (Figure 3.5) revealed the importance of a basic stabilization control structure that included controlling the oxygen and nitrate concentrations in the fish tank (Figure 3.6). Additionally, pH needs to be controlled in practice, and steady-state results in Tables 3.6-3.9 show four scenarios using base or buffer to control the pH in the biofilter. The optimal location of the base or buffer feed and the choice between the two require detailed analysis, as it depends on economic factors.

The proposed model demonstrated excellent performance when simulated using real data, resulting in a trajectory with high similarity to reality, considering the simplified nature of the model. However, to obtain more accurate carbon dioxide and nitrate levels, all losses of these quantities should be taken into account.

Overall, the proposed model is numerically robust and well-suited for further studies on optimal operation and control of RAS water treatment systems.

Chapter 4

Optimal Control of the Water Quality

It is important to have automated solutions to reduce variations and optimize operations. This chapter describes and presents three optimal control structures to achieve that while avoiding unnecessary costs and keeping the welfare of the fish. It is an extension of Paper II, which was published at the IFAC Symposium on Dynamics and Control of Process Systems (DYCOPS, 2022). The extensions mainly include the addition of figures and transfer functions that had to be omitted in the IFAC version due to space limitations.

4.1 Abstract

This study compares nonlinear model predictive controls, using setpoint tracking objective function (NMPC), and economic objective function (E-NMPC), with a hierarchical control structure of PI controllers applied to the water treatment of a Recirculating Aquaculture System (RAS), which consists of a tank, a biofilter, a stripper and an oxygen cone. Two of the three control structures used in this work consist of an optimization layer on top of proportional-integral (PI) control loops or NMPC. The optimization layer reduces the degrees of freedom with an economic objective function by deactivating some of the manipulated variables when choosing between buffer and base addition and the location of addition to the system. The third structure consists of a single layer with E-NMPC. The PI control structure is easy to design once we know the relationship between the variables. The PI controllers' performance was satisfactory, but a small back-off would be needed, if the constraints would not be soft constraints. Alternatively, the use of buffer with base would be necessary to improve speed and avoid

constraint violation, as one component took more than 6 days to reach the optimal concentration. The NMPC and the E-NMPC performed better: the NMPC was much faster in conducting the controlled variables to optimal conditions, despite not providing optimal economic cost during the trajectory; and the E-NMPC provided a mixture of smooth trajectory and optimal cost.

4.2 Introduction

Aquaculture systems for commercial purposes consist of rearing one or more species of aquatic organisms inshore or offshore. In inshore or offshore closed environments, the focus is usually on rearing only one species, as the conditions are controlled and external contact is avoided. The effluent is significantly larger in flow-through systems, which are also called raceways, due to the discharge of the entire outflow of the tank (Ridler and Hishamunda, 2001). A modification to raceways are recirculating of treated water, and these processes are called Recirculating Aquaculture Systems (RAS).

Automated RAS, also called Smart RAS or Intelligent Aquaculture consists of implementing control and optimization solutions to avoid risks and reduce production with as little as possible of human interaction with the system (Lee et al., 2020). This is a challenge due to the complexity of the system, but it is less difficult when the system is divided into subsystems: rearing unit, solid, and water treatments.

This study is focused on the water treatment part of Atlantic salmon (*Salmo salar*) RAS, which consists of a tank, a biofilter, a stripper, and an oxygen cone. The system is complex, but it was simplified in previous work (dos Santos et al., 2023), where a model was developed for control and optimization purposes, the steady state and dynamic behaviors were analyzed, and simple proportional integral control of oxygen and nitrate were implemented. For optimal growth and welfare of the fish, the conditions of the environment are assumed to have a small range, so other controllers are required to keep them within this region.

Other authors have applied control and optimization to other RAS configurations, including Wright (2011), Farghally et al. (2014), and Summerfelt et al. (2015). In order for the control and optimization to be successful, one needs to gather information on all the toxic compounds, important water conditions, and all the safety bounds. When the system operates in optimal conditions, one is able to distinguish which constraints affect the optimization directly or indirectly, as they are active or not. The inactive constraints are important to the dynamic optimization to avoid abrupt changes and going too far from optimal steady-state conditions, and the active ones dictate these conditions.

The main contribution of this work is the comparison of nonlinear model

predictive control structures with a systematic procedure for control design applied to a water treatment system of a recirculating aquaculture system of Atlantic salmon.

4.3 Process description

The process, illustrated in Fig. 4.1, consists of a tank, where the fish is reared, and a water treatment system. In the water treatment system, the tank effluent is treated by a biofilter, on which bacteria convert ammonium into nitrate, and a stripper, removes carbon dioxide from the system. Most of the effluent is recycled back to the tank, and the rest is purged. There are makeup streams of water and oxygen, and other inputs, such as air fanned through the stripper, fish feed added in the fish tank, and base (NaOH) and/or buffer ($NaHCO_3$) that can be added to the tank or to the biofilter.

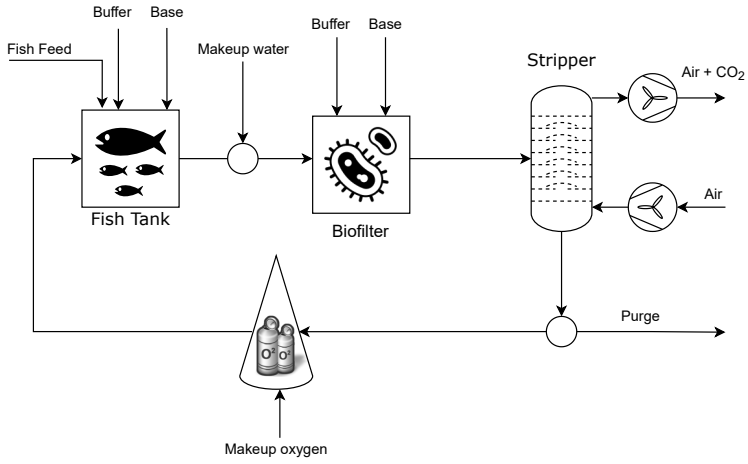

Figure 4.1: Process diagram.

The fish feed is considered a disturbance that changes from day to day in a piece-wise constant manner. Fish metabolism is considered to produce ammonia, carbon dioxide, and biomass, which is the mass growth of the fish, and their production rates are assumed to be linear functions of the fish feed. In the biofilter, bacteria are considered to transform ammonia (NH_3) into nitrate (NO_3^-) with a constant conversion. The temperature and salinity are assumed to be constant and equal to 14°C and 15 g/kg, respectively.

The model uses three reactions invariant variables, which are variables that do

not change with equilibrium reactions, and these variables are defined as follows:

$$c_{TAN} = c_{NH_3} + c_{NH_4^+} \tag{4.1}$$

$$c_{TIC} = c_{H_2CO_3} + c_{HCO_3^-} + c_{CO_3^{2-}} \tag{4.2}$$

$$c_{alk} = c_{OH^-} + c_{HCO_3^-} + 2c_{CO_3^{2-}} - c_{NH_4^+} - c_{H^+} \tag{4.3}$$

where c_j is the concentration of component j, TAN denotes total ammonia nitrogen, TIC is total inorganic carbon, and alk is alkalinity.

Other differential states are nitrate and oxygen concentrations in the tank and biofilter, and the algebraic states are TIC concentration in the stripper and pH in all units. The model consists of 14 differential and algebraic equations. More details about the process and model can be found in Chapter 3 or in dos Santos et al. (2023).

4.4 Optimization Problem

4.4.1 Operating constraints

The system must satisfy a few constraints to keep the fish safe, healthy, and in optimal growth rate conditions. Depending on the species and size of the RAS, these constraints differ. Pedersen (2018) exemplifies an optimization of RAS design for Rainbow trout and Atlantic salmon, where it cites different parameters depending on the species. As the fish species in this work is Atlantic Salmon, the restrictions for optimal growth rate and safety regarding w_i, which is the mass concentration of component i, pH, and alkalinity are given as follows:

- Carbon dioxide:
$$w^T_{H_2CO_3} \leq 15mg/L$$
- Nitrate:
$$w^T_{NO_3^-} \leq 100mg/L$$
- Ammonia:
$$w^T_{NH_3} \leq 20\mu g/L$$
- pH in the tank:
$$7 \leq pH^T \leq 7.5$$
- pH in the biofilter:
$$7 \leq pH^B \leq 8$$

- Alkalinity in the tank:

$$w_{alk}^{T} \geq 50mg(CaCO_3)/L$$

- Alkalinity in the biofilter:

$$w_{alk}^{B} \geq 50mg(CaCO_3)/L$$

There are also some operating constraints that are based on the size parameters described in 3 regarding oxygen mass concentration, $w_{O_2}^{T}$, recirculating volumetric flow rate, q, and maximum amount of air being ventilated through the stripper, $\dot{V}_{air}$.

- Oxygen concentration:

$$80\% \times w_{O_2,sat} \leq w_{O_2}^{T} \leq 120\% \times w_{O_2,sat}$$

  where $w_{O_2,sat}$ is the mass concentration of oxygen in water at saturation.

- Recirculating volumetric flow rate:

$$5m^3/min \leq q \leq 50m^3/min$$

- Air flow rate:

$$\dot{V}_{air} \leq 5q_{max}$$

4.4.2 Economic Objective Function

A general optimization problem is given by

$$\min_{\boldsymbol{x},\boldsymbol{z},\boldsymbol{u}} \; J(\boldsymbol{x},\boldsymbol{z},\boldsymbol{u}) \tag{4.4}$$

$$\begin{aligned} \text{s.t.} \quad & \dot{\boldsymbol{x}} = s_d(\boldsymbol{x},\boldsymbol{z},\boldsymbol{u}), \\ & s_a(\boldsymbol{x},\boldsymbol{z},\boldsymbol{u}) = 0, \\ & g(\boldsymbol{x},\boldsymbol{z},\boldsymbol{u}) \leq 0, \\ & \boldsymbol{x}(0) = \boldsymbol{x}_0 \end{aligned}$$

where functions s_d and s_a are the differential and the algebraic equations, respectively, g is the set of inequality constraints mentioned in the previous subsection, and x_0 is the initial condition.

Table 4.1: Price of each input and output

Variable	Value	Unit	Description
p_1	19.19	NOK/m^3	Effluent disposal
p_2	5.71e-05	NOK/mol	Vacuum and Exhaustion fans
p_3	0.102	NOK/mol	NaOH flakes
p_4	0.148	NOK/mol	$NaHCO_3$ powder
p_5	14.17	NOK/m^3	Makeup water
p_6	1.87e-02	NOK/m^3	Pump operation

As the model does not take the effect of water quality on the fish growth into consideration, the cost of the plant, *S*, which is also the function *J* to be minimized in a steady-state economic optimization in each step k, is purely given by the operating cost, given by Eq. 4.5. In the case of dynamic economic optimization, the corresponding cost function, *J*, becomes *S* plus the regularization term, as shown in Eq. 4.10, in the next section.

$$\begin{aligned} J = S(\mathbf{u}_k) = p_1(1-r)q^B + p_2\,\dot{m}_{air} + p_3 \sum_{i=T,B} \dot{m}^i_{base} \\ + p_4 \sum_{i=T,B} \dot{m}^i_{buffer} + p_5\,q^m + p_6\,q \end{aligned} \tag{4.5}$$

where p_j with $j = 1, 2, ..., 6$ are prices of operation of vacuum and exhaustion fans (Nistad, 2018); base (Tianjin Chengyuan Chemical CO. LTD, 2021); buffer (Farmasino CO. LTD, 2021); makeup water, which is assumed to have the same price as fresh water; effluent disposal (Trondheim kommune, 2021); and standard pump operation. The prices are listed in Table 4.1, it is assumed that they do not change during the operation. q is the recirculation flow rate, q^m is the makeup water, q^B is the water flow rate through the biofilter (which is calculated by the sum $q + q^m$), r is the recycling ratio (which is calculated by q/q^B), $\dot{m}_{air}$ is the air feed to stripper, $\dot{m}^i_{base}$ is the base feed to the unit i, $\dot{m}^i_{buffer}$ is the buffer feed to the unit i, and i can be T, B, or S, which are tank, biofilter and stripper.

4.5 Control Design

A summary of all structures is presented in Figure 4.2. Case A consists of an upper layer with a steady-state optimization, a middle layer with a Split-range block, and a lower layer with PI control. Case B consists of an upper layer with a steady-state optimization and a lower layer with nonlinear model predictive control

(NMPC). Finally, Case C consists of a single layer with economic model predictive control (E-NMPC).

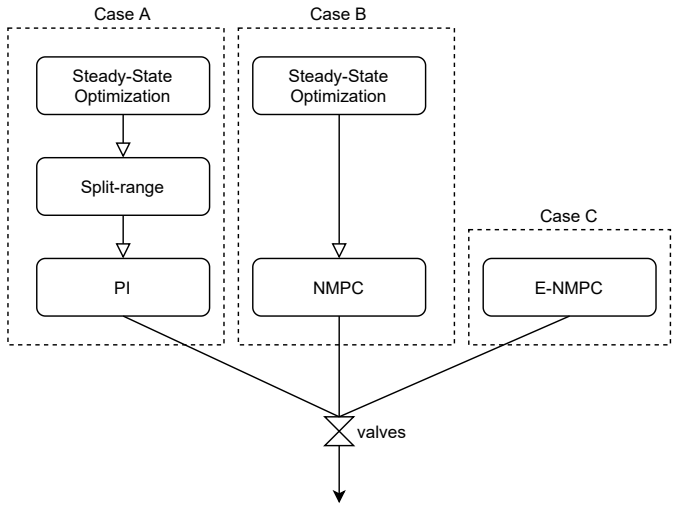

Figure 4.2: Control structures.

Another point is that the disturbance changes in a piece-wise constant manner dependent on the day of operation, and, thus, the system needs to be optimized daily for Cases A and B.

The simulation of the plant, which is represented by a first-principle model of the water treatment of RAS, uses IDAS method from SUite of Nonlinear and DIfferential/ALgebraic equation Solvers (SUNDIALS), distributed along with CasADi v3.5.5 for Python v3.8.8.

4.5.1 Case A

After formulating the optimization problem, the next steps are to optimize using Eq. (4.4) and (4.5) for expected disturbances and implement the optimal operation, defining what to control.

Based on the optimization result, the active constraints dictate the most important variables to be controlled, and its setpoint becomes the restriction value. The optimization also defines the location of base/buffer addition. In order to pass this optimal decision to the regulatory layer, a split-range block must be put in between to activate or deactivate the base/buffer addition, depending on the type and location.

In dos Santos et al. (2023), we showed that it is essential to control oxygen and nitrate concentrations. Based on that, the oxygen and nitrate pairings are set,

but process knowledge needs to be used to suggest other pairings. A systematic procedure is conducted for the remaining pairs to be defined.

4.5.1.1 Model identification:

First, the system is identified as a first order plus time delay (FOPTD) model. To achieve that, a step change is applied in one manipulated variable (u) at a time, and the identification of the dynamic responses is executed using the Scipy package in Python, minimizing the integral of the absolute magnitude of the error (IAE), subject to bound constraints, and described by the following equation:

$$\min_{\boldsymbol{t},\boldsymbol{y},k,\tau,\theta} \int_0^{t_f} |error(\boldsymbol{t},\boldsymbol{y},k,\tau,\theta)|dt \tag{4.6}$$

$$\begin{aligned} \text{s.t.} \quad & \theta \geq 0, \\ & \tau \geq 0 \end{aligned}$$

$$error(\boldsymbol{t},\boldsymbol{y},k,\tau,\theta) = k(1-\exp(-(\boldsymbol{t}-\theta)/\tau)) - \boldsymbol{y} \tag{4.7}$$

where $error$ is the error function described by Eq. 4.7 dependent on time, $\boldsymbol{t}$, gain, k, time constant, τ, and time delay, θ; $\boldsymbol{y}$ is the dynamic response vector; t_f is the duration of the dynamic response.

4.5.1.2 Closing the control loops:

After all pairings are set, the control loops are closed in an order, and the identification is re-executed every time one loop is closed. The order of the closure is told by prior knowledge of the system on how intensely one input variable can affect the other controlled variables besides its pair.

Finally, the SIMC rules (Skogestad, 2003) (Skogestad's PID settings) for systems described by first order plus time delay (FOPTD) transfer functions are used to tune the controllers. The transfer function of each pairing m is presented in the equation below.

$$\frac{y_m}{u_m} = k\frac{e^{-\theta s}}{\tau s + 1} \tag{4.8}$$

4.5.2 Cases B and C

When letting the algorithm decide the location of the addition of base/buffer, this decision can be added to a nonlinear model-based predictive control. In order to solve the minimization problem of the model predictive control, the integration method needs to be chosen carefully. For this system, which has a measured disturbance that varies from day to day, the integration method single shooting is not advised, and multiple shooting increases the computation time a lot. Therefore, the method direct collocation was used, and set to have one intermediate collocation point and to use a third-degree polynomial to interpolate within each control interval.

The objective function to be minimized is given as follows:

Case B) Setpoint Tracking:

$$J = \sum_{k=0}^{N-1} \left[||\boldsymbol{x}_k - \boldsymbol{x}_{opt}||_Q^2 + ||\boldsymbol{u}_k - \boldsymbol{u}_{k-1}||_R^2 \right] \tag{4.9}$$

where N is the ratio between control horizon and control interval; Q and R are diagonal matrices of dimension $nx \times nx$, and $nu \times nu$, respectively. Here, nx is the number of differential states, $\boldsymbol{x}$, and nu is the number of manipulated variables, $\boldsymbol{u}$; x_{opt} is the optimal steady state for the differential states, given by the upper layer; $||\boldsymbol{u}_k - \boldsymbol{u}_{k-1}||_R^2$ is the penalty of change in the manipulated variables, also called regularization term.

Case C) Economic Dynamic Optimization:

$$J = \sum_{k=0}^{N-1} \left[S(\boldsymbol{u}_k) + ||\boldsymbol{u}_k - \boldsymbol{u}_{k-1}||_R^2 \right] \tag{4.10}$$

where *S* is the cost function given by Eq. (4.5).

4.6 Results and Discussion

4.6.1 Steady-state Optimization

With the optimization problem defined in Section 4.4, steady-state optimization can be easily done. The results for the first day of the production are presented in Tables 4.2 and 4.3.

Table 4.2: Optimal operation data on day 1

Variable	Value	Unit
$\dot{m}_{air}$	1074.71	mol/min
q^m	0.99	m^3/min
$\dot{m}_{O_2}$	11.36	mol/min
$\dot{m}^T_{base}$	4.21	mol/min
$\dot{m}^B_{base}$	1.21	mol/min
$\dot{m}^T_{buffer}$	0.0	mol/min
$\dot{m}^B_{buffer}$	0.0	mol/min
q	9.07	m^3/min

Table 4.3: Optimal steady-state values for some variables on day 1 [mmol/L or -]

Variables	Tank	Biofilter	Stripper
c_{alk}	4.32	3.85	3.85
c_{TIC}	4.74	4.27	4.04
$c_{H_2CO_3}$	0.27	0.43	0.21
c_{TAN}	0.18	4.91e-03	4.91e-03
c_{NH_3}	8.09e-04	1.21e-05	2.40e-05
$c_{NO_3^-}$	1.61	1.61	1.61
c_{O_2}	0.35	1.01e-06	1.01e-06
pH	7.26	7.0	7.3

The optimization results in Table 4.2 indicate that only base should be to the system. However, by manipulating the price of buffer, this could change, as illustrated in Figure 4.3 in the region in the middle (between 0.005 and 0.04 NOK/mol, approximately), where base and buffer are needed. The figure illustrates the trade-off between price and process requirement, and shows a range of buffer prices that activates the upper bound constraints of alkalinity and/or TIC concentration (range between 0 and 0.005 NOK/mol, approximately); a second region in the middle, where base is added in the tank, and buffer is added in the biofilter, referenced in this work as Case A.1; and a third region with only base being used, referenced as Case A.2. The current price of buffer lies in the third region, as seen from Table 4.1. The figure also shows that the addition of buffer in the tank is not recommended to reach steady-state optimum conditions, as the blue line lies under the others always marking 0 mol/min (zero).

Table 4.4 shows the operating constraints converted to the units of the system

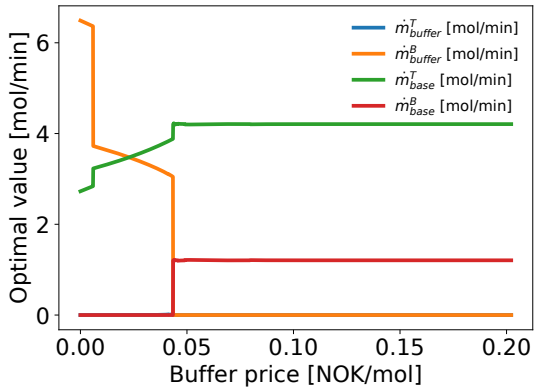

Figure 4.3: Buffer price sensitivity.

for better visualization. Comparing it with Table 4.3, we can see that the constraints are active for $c^T_{O_2}$ and $c^T_{NO_3^-}$, so they are chosen to be controlled variables. The other controlled variables are defined using process knowledge.

Table 4.4: Upper and lower constraints [mmol/L or -]

Lower bound	Variables	Upper bound
0.50	c^T_{alk}	-
0.50	c^B_{alk}	-
0	$c^T_{H_2CO_3}$	0.34
0	$c^T_{NH_3}$	0.0012
0	$c^T_{NO_3^-}$	1.61
0.24	$c^T_{O_2}$	0.35
7.0	pH^T	7.5
7.0	pH^B	8.0

4.6.2 PI Control Design

In order for the fish to have an optimal growth rate, the environment is required to satisfy a few constraints. Besides oxygen and nitrate concentrations, other restricted variables have a direct correlation with input variables, such as ammonia concentration, which depends on TAN concentration and pH; carbon dioxide, which depends on TIC concentration and pH; and pH, which is defined by alkalinity, TAN and TIC concentrations.

To reduce the number of controllers and reduce the nonlinearity of the relationship between MV and CV, alkalinity, TAN, and TIC concentrations are studied to be substituted for direct controls of carbon dioxide, ammonia, and pH. TAN concentration in the biofilter is defined by the biofilter efficiency, which is considered constant, TAN concentration in the tank, which depends linearly on the fish feed according to the fish metabolism assumption, and the liquid flow rate, q, which dictates how fast the water treatment is. Therefore, TAN concentration in the tank needs to be controlled and its pair should be q, as the fish feed is a disturbance.

Alkalinity and TIC concentrations (in the tank and in the biofilter) can be controlled by the MVs left: the amount of base or buffer added in the tank and in the biofilter, and the amount of air used for the stripper. TIC concentration in the biofilter just changes with TIC concentration in the tank, recirculating volumetric flow rate, q, makeup water, and air inlet. Therefore, one of the TIC concentrations needs to be controlled by the air inlet, and the closest one from the stripper is TIC concentration in the tank.

The bounded optimization solved to identify the responses was very sensitive to the initial guess. Therefore, dynamic response graphs, which can be seen in Figure 4.4, are important to set good initial guesses.

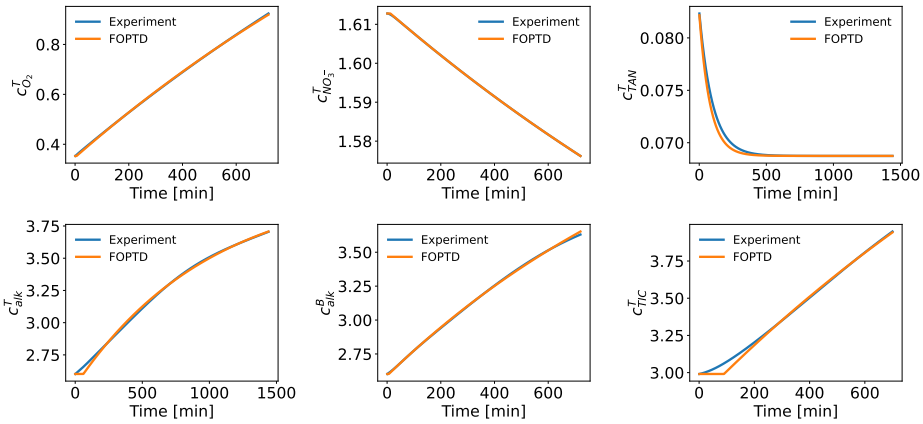

Figure 4.4: FOPTD identification of the controlled variables. The simulated behavior is in blue, while the predicted behavior using an FOPTD function is in orange.

Using the knowledge from the process acquired in previous work and choosing the closest pair, the pairing is chosen as in Table 4.5, although the controller using buffer is deactivated on day 1, it can be activated as needed by the Split-range block. The step values applied to the manipulated variables are given in Table 4.6.

Table 4.5: Suggested pairing and tuning parameter

MV	CV	τ_C
$\dot{m}_{O_2}$	$c^T_{O_2}$	15.46
q^m	$c^T_{NO_3^-}$	22.25
q	c^T_{TAN}	1000.0
$\dot{m}^T_{base}$	c^T_{alk}	645.38
$\dot{m}^B_{base}$	c^B_{alk}	153.72
$\dot{m}^B_{buffer}$	c^B_{alk}	-
$\dot{m}_{air}$	c^T_{TIC}	1900.0

Table 4.6: Step values applied to the MVs

MV	Step value [%]
$\dot{m}_{O_2}$	20
q^m	10
q	20
$\dot{m}^T_{base}$	50
$\dot{m}^B_{base}$	5
$\dot{m}^B_{buffer}$	-
$\dot{m}_{air}$	10

To each line m of Table 4.5, the transfer function was identified. They are given by:

$$\frac{y_1}{u_1} = 0.82\frac{e^{-5.46s}}{2000s+1} \tag{4.11}$$

$$\frac{y_2}{u_2} = -1.48\frac{e^{-12.18s}}{2476.75s+1} \tag{4.12}$$

$$\frac{y_3}{u_3} = -0.003\frac{e^{-1.41E-09s}}{80s+1} \tag{4.13}$$

$$\frac{y_4}{u_4} = 0.71\frac{e^{-60.77s}}{1009.39s+1} \tag{4.14}$$

$$\frac{y_5}{u_5} = 11.98\frac{e^{-6.38s}}{1311.98s+1} \tag{4.15}$$

$$\frac{y_6}{u_6} = -0.004\frac{e^{-90s}}{2000s+1} \tag{4.16}$$

The order of closing the loops affects the difficulty of controlling the system, meaning that some CVs are coupled with more than one manipulated variable, as expected, but this problem can be bypassed if the loops that affect other variables the most are closed before. The order of closure of the loops, and the tuned $\boldsymbol{\tau_C}$, which is a vector of the variables to be tuned in each control when using the SIMC rules, are also shown in the table below. The PI control structure of the process can be seen in Figure 4.5 for better visualization.

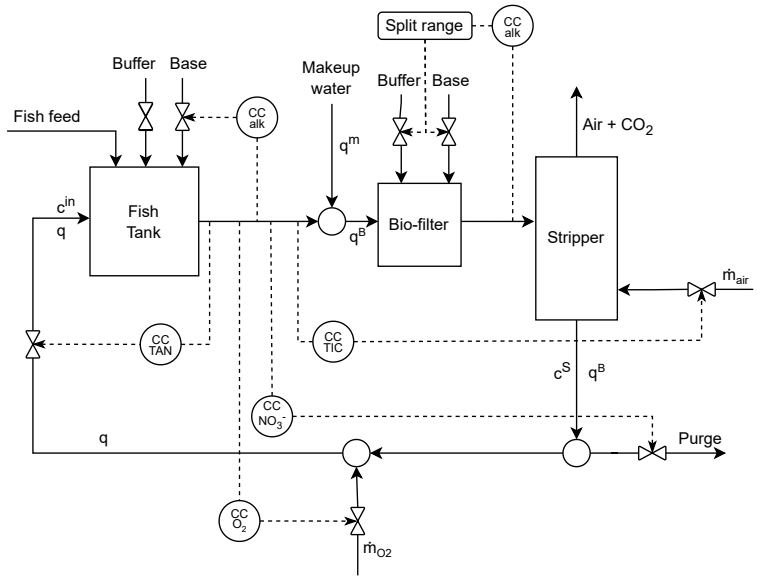

Figure 4.5: PI control structure of Case A.2.

4.6.3 Dynamic Simulation with PI controllers

The system has 8 dynamic degrees of freedom, but with the optimization results no buffer is needed, in this case. Therefore, 6 controllers need to be active.

Figure 4.6 shows the main dynamic responses to step changes in the disturbance with only oxygen and nitrate being controlled. Almost all variables violate the constraints, leading the fish to suffer, and causing non-optimal growth or death. Figure 4.7 shows the main CVs' dynamic responses to the same disturbance step changes. From this figure, it can be seen that one CV (c_{TIC}^T) does not reach the setpoint within 6 days, and the controller could not have been any

faster due to abrupt changes and constraint violation of other variables, such as pH. Alternatively, a small back-off would be needed, or to use buffer at the beginning, when there is a need for an abrupt increase in base intake. The latter alternative could lead the system to optimal conditions quicker, as the pH would not violate the constraints and alkalinity would increase faster with more base/buffer.

Overall, the closed loops performed well, and almost the entire system was driven to optimal steady-state conditions eventually, being c^T_{TIC} the only variable that did not reach optimal steady-state conditions. The pH constraint violation does not guarantee an optimal growth condition during the violation period, which might not lead to the best option as a control structure.

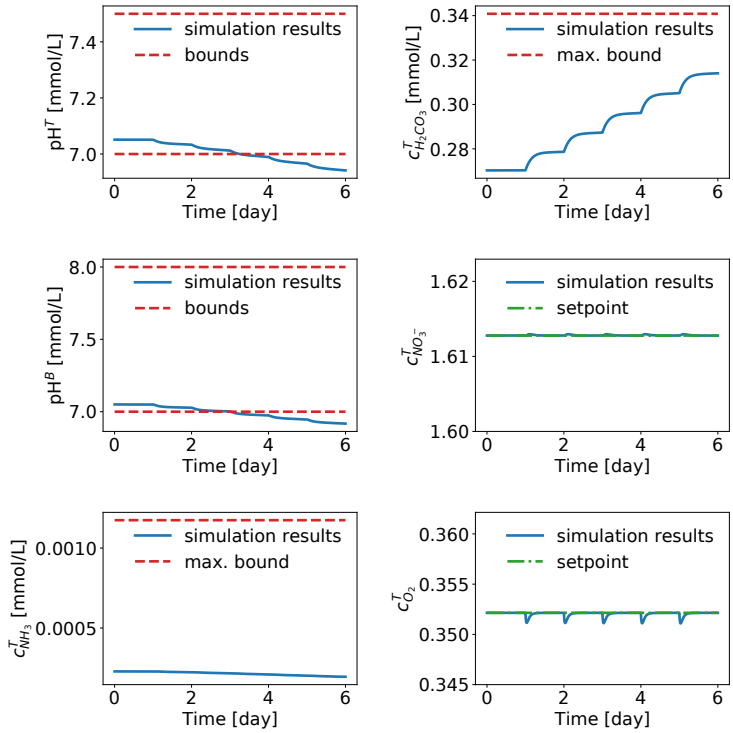

Figure 4.6: Dynamic behavior of the process with oxygen and nitrate controls, and subject to disturbance F

4.6.4 Model Predictive Control comparison

Two different objective functions for the optimal controllers were used: setpoint tracking and economic objective function, described by Eq. (4.9) and

(4.10), respectively. The tuned diagonal matrices Q and R are given as follows:

$$Q = diag(1e2, 1e2, 1e3, 1e3, 1e2, 1e2, 1, 1, 1, 1)$$
$$R_{\text{NMPC}} = diag(1e{-}3, 1e3, 1e2, 1e2, 1e2, 1e2, 1e2, 1e2)$$
$$R_{\text{E-NMPC}} = diag(1e{-}7, 10, 1, 1e{-}3, 1e{-}4, 1e{-}4, 1e{-}4, 10)$$

Figure 4.7 shows the closed loop response with a control horizon of 24 hours and control interval of 20 minutes, for all cases. The NMPC conducted all controlled variables to their optimum values plus algebraic variables in a really short time (less than a day). The E-NMPC performed well also, although it took more time for the CVs to reach optimal steady-state value. The input values are presented in Figure 4.8.

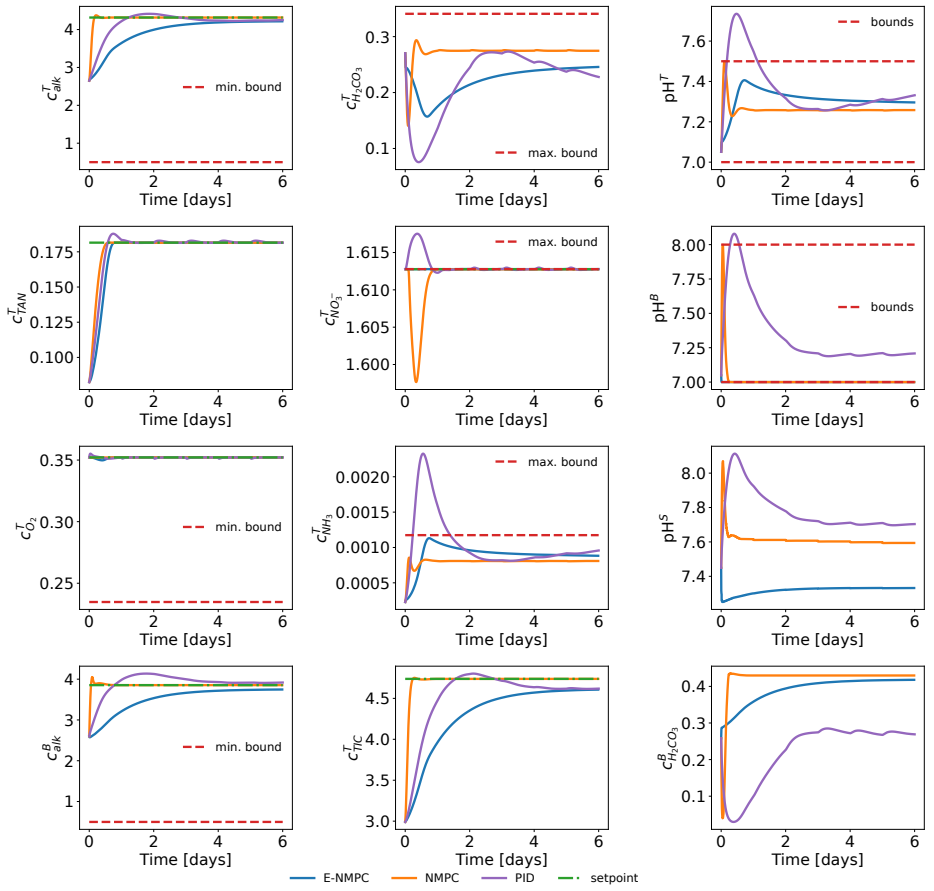

Figure 4.7: Dynamic behavior of the CVs of the 3 cases, subject to disturbance F.

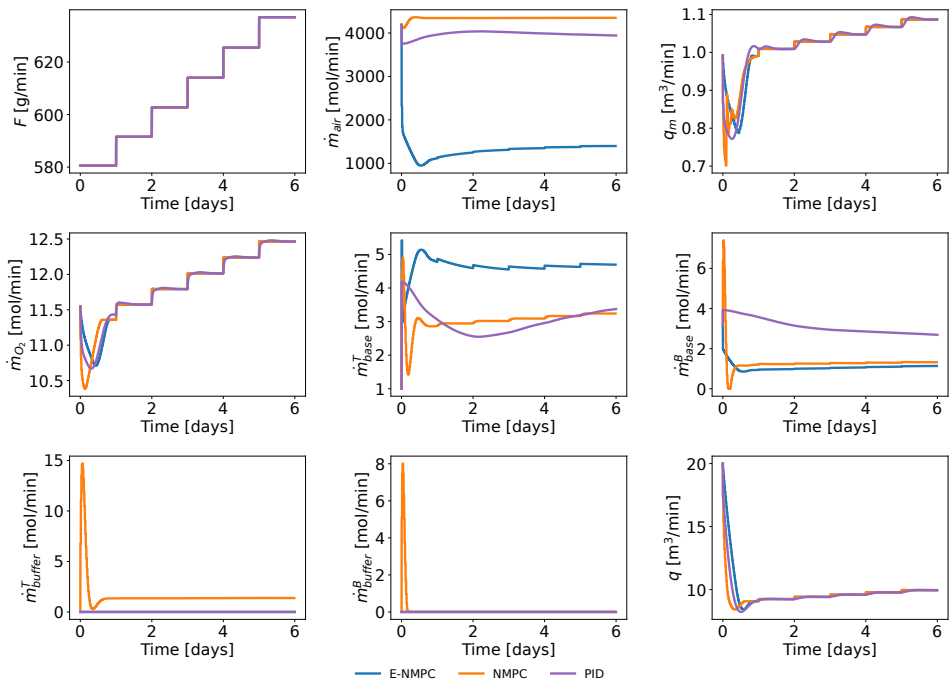

Figure 4.8: Dynamic behavior of the inputs of the 3 cases, where F is the disturbance.

4.7 Conclusion

The volumes of the different RAS units are large, except for the stripping column, causing the time constant of the entire process to be high. On the other hand, the disturbance can lead the process to infeasibility, if no control is done. To speed up the process and avoid infeasibility, a control structure is needed.

In this work, we have presented a comparison of three optimal control structures. Two of them are hierarchical control structures, where an optimization layer calculates the optimal setpoints. In Case A, after the optimization layer, a split-range block handles the switch between manipulated variables. In Case B, the optimization layer gives the optimal setpoint directly to a nonlinear model predictive controller. In Case C, the structure is a single block consisting of an economic model predictive control, led by an economic objective function.

All the control structures gave a satisfactory performance, driving the system to the optimal steady-state conditions. The PI control structure depends on how far from optimal the system is at the beginning to drive it faster to optimal conditions, as it took more than 6 days to reach optimality. To make the PI controllers faster, buffer would be needed, which means that it would cost more, as buffer

is more expensive than base, according to the current prices. The E-NMPC provided a trajectory that is economically optimal, but it achieves a different steady-state optimum. On the other hand, the NMPC provided a dynamically optimal trajectory, but also economically non-optimal, as it uses both buffer and base. Comparing NMPC with the PI controllers, the NMPC performance was faster in driving the system to optimal steady-state condition, as it uses buffer and base. The trade-off between speed and cost is evident, but E-NMPC gave the best trajectories, pushing the system to an optimal condition at a lower cost.

All the control structures were designed and tested using computational simulations and the model presented in previous work. Therefore, an implementation of these structures controlling the system with growth rate variation and addition of noise is suggested to evaluate the effect of model mismatch on the results.

4.8 Discussion of Paper II - Optimal Control of Water Quality in a Recirculating Aquaculture System

This chapter described the development of control structures and optimization of a RAS process. The model did not consider the effect of fish growth on fish metabolism, but this effect might not be negligible for the optimization problem. The next chapter presents a reformulation of the optimization problem considering this effect and other real-life limitations.

Chapter 5

Real-Life Limitations for Optimal Control of Water Quality

This chapter presents the imposition of real-life limitations on some input variables and the reformulation of the optimization problem.

5.1 Reformulation of the Objective Function

The developed model in Chapter 3 does not take into consideration the effect of water quality on fish growth, but, in reality, this effect might not be negligible. To account for that, the cost of the plant, S was reformulated as

$$\begin{aligned} S(\mathbf{u}_k) =& p_1(1-r)q^B + p_2\,\dot{m}_{air} + p_3 \sum_{i=T,B} \dot{m}^i_{base} \\ &+ p_4 \sum_{i=T,B} \dot{m}^i_{buffer} + p_5\,q^m + p_6\,q + p_7 F - p_8 G \end{aligned} \tag{5.1}$$

where p_j with $j = 1, 2, ..., 6$ are essentially the same prices described in Table 4.1, except that fish feed, F, and biomass, G, sale prices have been added, with j now going up to 8. The updated table is presented below (Table 5.1).

5.2 Water flow rate and CO_2 limitations

In order to approach real-life conditions, some constraints need to be changed. One of them is the range of the recirculation flow rate, which is more limited

Table 5.1: Price of each input and output

Variable	Value	Unit	Description
p_1	19.19	NOK/m^3	Effluent disposal
p_2	5.71e-05	NOK/mol	Vacuum and Exhaustion fans
p_3	0.102	NOK/mol	NaOH flakes
p_4	0.148	NOK/mol	$NaHCO_3$ powder
p_5	14.17	NOK/m^3	Makeup water
p_6	1.87e-02	NOK/m^3	Pump operation
p_7	0.018	NOK/g feed	Fish feed
p_8	0.061	NOK/g fish	Fish biomass sale

in real-life conditions due to events that were not considered when developing the model, such as sedimentation in pipes and fish swimming requirements. To avoid these events, a minimum opening of 70% of the recirculation flow valve is required, which determines a new q_{min}. With this limitation, the maximum opening is set to the optimum value calculated on the last day of RAS rearing (day 90), $q_{opt_{90}}$. The new constraint is then given as

$$0.7\ q_{opt_{90}} \leq q \leq q_{opt_{90}}$$

Another deviation from the real-life conditions is that the air flow rate is kept constant throughout the rearing period at the optimal value of the last day. These two real-life conditions reduce the number of DoFs by two, leaving the oxygen inlet, the makeup water, and base/buffer feed as the remaining DoFs. As the oxygen inlet and the makeup water are used to stabilize oxygen and nitrate levels, there is only one degree of freedom left at a steady state from day 1 to the day when the optimal q is equal or higher than $0.7\ q_{opt_{90}}$.

The effect of CO_2 on the fish growth is also not negligible in reality (Khan et al., 2018). Khan *et al.* studied this relationship by executing experiments with varying CO_2 exposure over the same amount of days to different groups of fish. The authors found out that the concentration of dissolved CO_2 affects negatively the growth by approximately 10% for the mentioned range of dissolved CO_2 concentration. This relationship can be represented by changing the assumption of optimal and constant feed conversion ratio (FCR) to an apparent FCR (aFCR) linearly dependent on the CO_2 concentration. Therefore, two equations were added to the model:

$$aFCR = 0.009 MM_{CO_2} \times c^T_{H_2CO_3} + 0.97 \tag{5.2}$$

$$G = F/aFCR \tag{5.3}$$

where $c^T_{H_2CO_3}$ is in [mmol/L], MM_{CO_2} is the molar mass of CO_2 in [g/mol] and G is the growth rate in [g/min].

5.3 Results and Discussion

Optimizing the process on day 90 (the last day of rearing) gives new bounds for the recirculation flow rate:

$$q_{opt_{90}} = 39.82$$
$$0.7 q_{opt_{90}} = 27.87$$
$$27.87\ m^3/min \leq q \leq 39.82\ m^3/min$$

On day 52, q_{opt} is equal to 28.03m^3/min, which is slightly higher than the minimum value. This means that the process can operate at optimal conditions from day 52 to day 90.

Optimal costs, active constraints, and how far we are from it are calculated in order to analyze the optimization problem. It is shown in Tables 5.2-5.5 on three different days: day 1, day 52 and day 90. Tables 5.2 and 5.3 show the results for the new formulation with old constraints, named as Case 1; and Tables 5.4 and 5.5, the new formulation with new q and $\dot{V}$ constraints, named as Case 2.

Case 1: old q and $\dot{V}$ constraints

Table 5.2: Optimal operational data of Case 1

Variable	Day 1	Day 52	Day 90	Unit
$\dot{m}_{air}$	5682.63	10474.75	10474.75	mol/min
q^m	0.99	2.29	3.61	m^3/min
$\dot{m}_{O_2}$	11.43	26.4	41.53	mol/min
$\dot{m}^T_{base}$	4.32	10.31	17.28	mol/min
$\dot{m}^B_{base}$	0.0	0.0	0.0	mol/min
$\dot{m}^T_{buffer}$	0.0	0.0	0.0	mol/min
$\dot{m}^B_{buffer}$	0.0	0.0	0.0	mol/min
q	12.88	28.03	39.82	m^3/min

Table 5.3: Constraint analysis of Case 1 in [mmol/L or -]

Lower bound	Variable	Day 1	Day 52	Day 90	Upper bound
-	$c^T_{H_2CO_3}$	0.11	0.12	0.13	0.34
-	$c^T_{NH_3}$	9.92e-04	1.05e-03	1.17e-03	1.17e-03
-	$c^T_{NO_3^-}$	1.61	1.61	1.61	1.61
0.23	$c^T_{O_2}$	0.32	0.33	0.33	0.35
0.5	c^T_{alk}	3.09	3.25	3.61	-
0.5	c^B_{alk}	2.75	2.88	3.17	-
7.0	pH^T	7.5	7.5	7.5	7.5
7.0	pH^B	7.0	7.0	7.0	8.0

Case 2: new q and $\dot{V}$ constraints

Table 5.4: Optimal operational data of Case 2

Variable	Day 1	Day 52	Day 90	Unit
$\dot{m}_{air}$	10474.75	10474.75	10474.75	mol/min
q^m	0.99	2.29	3.61	m^3/min
$\dot{m}_{O_2}$	11.56	26.4	41.53	mol/min
$\dot{m}^T_{base}$	3.83	10.31	17.28	mol/min
$\dot{m}^B_{base}$	0.0	0.0	0.0	mol/min
$\dot{m}^T_{buffer}$	0.0	0.0	0.0	mol/min
$\dot{m}^B_{buffer}$	0.0	0.0	0.0	mol/min
q	27.87	28.03	39.82	m^3/min

Table 5.5: Constraint analysis of Case 2 in [mmol/L or -]

Lower bound	Variable	Day 1	Day 52	Day 90	Upper bound
-	$c^T_{H_2CO_3}$	0.08	0.12	0.13	0.34
-	$c^T_{NH_3}$	4.59e-04	1.05e-03	1.17e-03	1.17e-03
-	$c^T_{NO_3^-}$	1.61	1.61	1.61	1.61
0.23	$c^T_{O_2}$	0.32	0.33	0.33	0.35
0.5	c^T_{alk}	2.39	3.25	3.61	-
0.5	c^B_{alk}	2.25	2.88	3.17	-
7.0	pH^T	7.5	7.5	7.5	7.5
7.0	pH^B	7.16	7.0	7.0	8.0

These results show that, with the new formulation, the pH^T constraint becomes active, and the fish is less exposed to higher H_2CO_3 concentration as the range of recirculation flow rate is narrower, giving faster and smaller deviations on the water treatment. With the new constraints, the optimal correction of pH is done by adding base to the fish tank only, but this is still dependent on the base and buffer prices.

Chapter 6

Soft Sensor of Key Components, using Feedforward Networks

In this chapter, the authors intended to test the capabilities of an automatic neural network search tool (neural architecture search tool) and test how well a feedforward neural network model would represent a nonlinear model such as the steady-state RAS model. It presents a machine-learning application for monitoring important concentrations of a Recirculating Aquaculture System. It does not aim to find the best model for the application, but a better alternative to manual sampling. It is the same as Paper III, which was published in Computer Aided Chemical Engineering journal.

6.1 Abstract

Recirculating Aquaculture Systems are known to have their water quality conditions controlled, despite being common to have a simple control structure and a lot of human interaction to achieve that. To avoid long-term exposure to toxic levels of carbon dioxide and ammonia, its concentration needs to be monitored more often than manual measurements normally allow. In this work, we analyze the multilayer perceptron's ability to monitor water quality components that are important for the development of the fish. This alternative method for monitoring has the potential to complement the current sensor structure and laboratory procedures for manual measurement collection, but more studies need to be done on the type of machine learning model.

6.2 Introduction

Recirculating Aquaculture Systems (RAS) have two dynamic sub-systems: fish metabolism and water treatment. The water treatment system is responsible for keeping the water quality at high standards, reducing water consumption, and reducing contact with external pathogens (European Market Observatory for Fisheries and Aquaculture Products, 2021).

Regarding water quality, some components are important to be monitored and controlled due to toxicity but are hard or not able to be measured continuously, such as ammonia. In addition, it requires either several sensors or a central sensor station with a sampling system to get information about the levels of dissolved carbon dioxide and ammonia in all fish tanks and water treatment systems. One way of using information about the process to estimate the concentration of these toxic components is by using soft sensors (Fortuna et al., 2007).

The soft sensor technique is a combination of data, for parameter estimation, and process knowledge, for feature selection. The development of the data-driven models can be done, for example, using machine learning models, such as feedforward neural networks (FNN). In this work, the main objective is to apply multilayer perceptron (MLP) (Werbos, 1974), which is a classic type of FNN and a universal approximator (Hornik et al., 1989), as a soft sensor for recirculating aquaculture of Atlantic salmon (*Salmo salar*).

In RAS, even if fish, feed, and waste production increase in an exponential way, the goal is that the water quality should be kept stable and good. Measurements of ammonia are performed manually daily, whereas CO_2 is measured continuously at least at one point in the system. However, their levels might vary during the day depending on feeding and other factors, and data about this may be missed. Optimizing the water quality and fish growth would be easier with a higher resolution of information. In addition, manual collection and laboratory analyzes are time-consuming and therefore costly. Therefore, it is useful to develop an alternative method to monitor these water quality variables.

As the system is assumed to reach a steady state after each day, the water treatment system is approximated to a steady-state model developed in previous work (dos Santos et al., 2023). The training and validation data are acquired from this model, where some parameters are considered uncertainties. To improve the soft sensor identification, the uncertainties are changed using Latin hypercube sampling (LHS) (Jin et al., 2005), so it contains the operating region, which provides conditions for fish optimal growth. After the addition of white noise, the data is used to train different MLP configurations for predicting carbon dioxide, ammonia, and ammonium concentrations.

6.3 Process Description

Figure 6.1 shows a diagram of the RAS this work is focused on. The process consists of a fish tank, a biofilter, a stripper, and an oxygen cone. The model is a simplified version of the process, as it does not consider the effect of the water quality on the fish metabolism if the conditions are kept within bounds. This assumption is reasonable for each phase of the fish life, which can last from weeks to years depending on a lot of factors. Therefore, this work is only valid for the phase the model represents, which is the smolt phase. This could be easily extended to other phases by changing some parameters in the model, such as the amount of product generated by the fish metabolism per kg of fish feed.

The measurements that are available from sensors or additions include recirculating volumetric flow rate, q; pH; fish feed rate, F; buffer additions, $\dot{m}_{buffer}$; base additions, $\dot{m}_{base}$; makeup water, q^m; air inlet flow rate, $\dot{m}_{air}$; makeup oxygen, $\dot{m}_{O_2}$; average salinity, S; average temperature, T. More details about the process can be found in dos Santos et al. (2023).

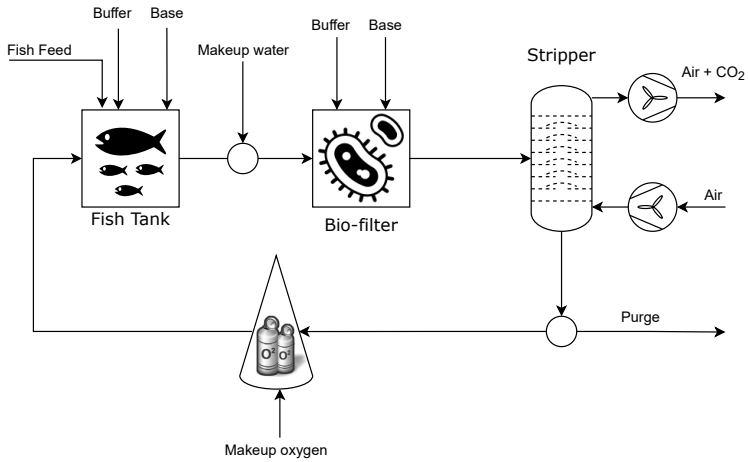

Figure 6.1: Process diagram of a recirculating aquaculture system.

6.4 Methodology

In order to develop a soft sensor, a standard procedure was followed. First, data was gathered, then preprocessed and divided into training and validation data. After that, the model was fitted to the data, and the best model was chosen for the validation. Finally, the model was tested with industrial data.

6.4.1 Training and Validation Data Acquisition

For the training and validation data acquisition, 6967 steady-state data points were generated within the region described by Table 6.1, using CasADi v3.5.5 (Andersson et al., 2019) in Python v3.8.8. 5967 of these data points were generated using latin hypercube sampling (LHS) built in `pyDOE` package in Python. LHS is a popular algorithm for planning computer experiments covering the entire range of uncertainties and disturbance in an optimally and distributed way for training. The rest was generated randomly within the same region for validating the soft sensor. After that, 1% white noise was added to both the input and output data of both training and validation data.

Table 6.1: Region of operation

Parameter	Mean	Unit	Range	Description
G/L	2.7	-	$\pm$ 50%	Gas-liquid ratio in equilibrium over the stripper
ξ_B	0.75	-	$\pm$ 25%	Biofilter efficiency
T	14	°C	$\pm$ 30%	Average temperature of the system
pH^m	7.0	-	$\pm$ 10%	pH of the makeup water
$y^{in}_{CO_2}$	4.15e-04	-	$\pm$ 10%	CO_2 composition in the air inlet
S	15.95	ppt	$\pm$ 30%	Average salinity of the system
pH^B_{des}	7.2	-	$\pm$ 1%	Desired pH for the biofilter
q	20	m^3/min	$\pm$ 50%	Recirculating volumetric flow rate
F	580.6	g/min	+ 50%	Fish feed rate

6.4.2 Data Preprocessing

Some concentrations are very low in RAS, when compared with other concentrations. Therefore, it is essential that all data is submitted to preprocessing. As the soft sensor model applied in this work is a deep learning neural network, the normalization of the datasets uses a minmax calculation of the training dataset. After that, the datasets are ready to be used to train and validate the soft sensor.

6.4.3 Soft Sensor

The feedforward neural network (FNN) architectures were created and optimized using the Auto-keras package (Jin et al., 2018), which is a package in Python that automatizes the neural architecture search (NAS) of models supported by another Python package named Keras.

In this work, the FNNs are multilayer perceptron (MLP), trained using the backpropagation method with a batch size of 500 samples. The objective function of the NAS was the validation loss, where the loss function was the mean squared error, and the maximum number of trials was 50. The features were chosen based on knowledge of the process and the available measurements in a real RAS.

After choosing the model with the lowest validation loss, the MLP performance was tested predicting the target concentrations from real data. To avoid breaking the non-disclosure agreement, the collected industrial data was normalized. The performances were compared using the root mean squared error between the scaled predicted and collected data.

6.5 Results

The choice of inputs was based on the available measurements from sensors or manual insertion of inlet streams described in the previous section. Three types of models were tested: multiple-input, single-output MLP (MISO-MLP), multiple-input, multiple-output MLP (MIMO-MLP), and a hybrid model, which consists of a MIMO-MLP predicting ammonium and dissolved CO_2 concentrations with ammonia concentration being calculated using the equilibrium equation, see Eq. (6.1).

$$c^T_{NH_3} = \frac{K_3(S,T)\, c^T_{NH_4^+}}{c^T_{H^+}} \tag{6.1}$$

where the equilibrium constant, K_3, is dependent on salinity and temperature, and the concentrations unit is mmol/L.

The inputs of the models were the same for MISO-MLP$_{NH_4^+}$ and MISO-MLP$_{NH_3}$ models: fish feed rate, F, recirculating volumetric flow rate, q, and pH in the tank, pH^T. The MIMO-MLP, MISO-MLP$_{H_2CO_3}$ and the hybrid models' features included the same as the previous with the addition of a new feature: air inlet flow rate, $\dot{m}_{air}$.

Figure 6.2 shows the prediction of the validation data using the MISO-MLP models, and Figure 6.3 shows the results using the hybrid model, and Figure 6.4 shows the results using the MIMO-MLP model. Comparing Figures 6.2 and 6.3, predictions of ammonium and dissolved carbon dioxide were similar, but ammonia predictions are worse using the hybrid model. Comparing Figures 6.2 and 6.4, the prediction of ammonia is slightly worse on the extremes using MIMO-MLP, and the other predictions were similar.

In Table 6.2, we summarize the performance of the models at the validation phase using the RMSE index. The best MLP architecture for this case study was

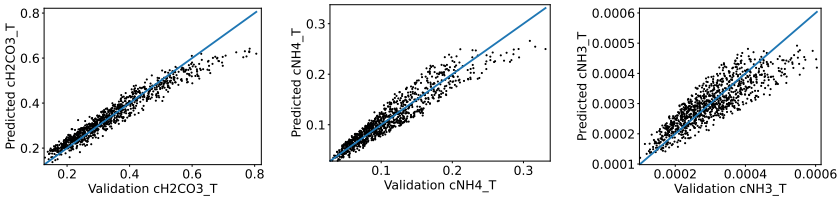

(a) Prediction of $c^T_{H_2CO_3}$ **(b)** Prediction of $c^T_{NH_4^+}$ **(c)** Prediction of $c^T_{NH_3}$

Figure 6.2: Prediction of validation data using the MISO-MLP models separately

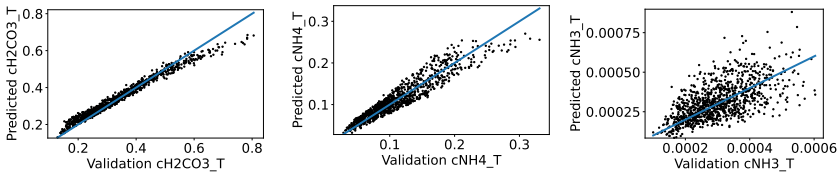

(a) Prediction of $c^T_{H_2CO_3}$ **(b)** Prediction of $c^T_{NH_4^+}$ **(c)** Prediction of $c^T_{NH_3}$

Figure 6.3: Prediction of validation data using the hybrid model

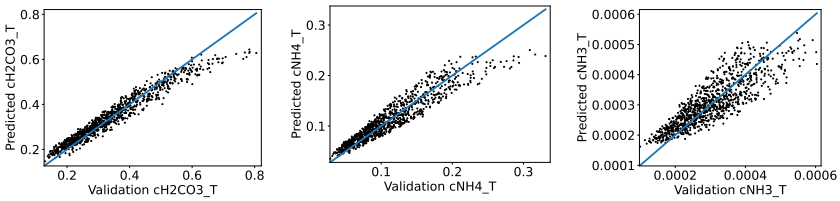

(a) Prediction of $c^T_{H_2CO_3}$ **(b)** Prediction of $c^T_{NH_4^+}$ **(c)** Prediction of $c^T_{NH_3}$

Figure 6.4: Prediction of validation data using the MIMO-MLP model

the MISO-MLP models put together, which gave the lowest final RMSE at the validation phase, and MIMO-NLP model was the second best giving similar, but slightly higher, RMSE.

Table 6.2: Summary of the models performance at the validation phase - RMSE index

Output	MISO-MLPs	Hybrid	MIMO-MLP
$c^T_{H_2CO_3}$	0.0645	0.0787	0.0694
$c^T_{NH_4^+}$	0.1204	0.1201	0.1230
$c^T_{NH_3}$	0.1322	0.2611	0.1351
Final	0.1097	0.1720	0.1129

The architecture of the MLPs is described in Table 6.3. MISO-MLP$_{H_2CO_3}$ model has two dense hidden layers with 32 nodes each using the rectified linear activation function (ReLU), while the others have one dense hidden layer, but with 64 and 128 nodes using the same activation function on MISO-MLP$_{NH_4^+}$ and MISO-MLP$_{NH_3}$ models, respectively. Note that ammonia concentration turned out to be harder to estimate when compared with ammonium, and possibly the NAS found a flat optimum, which means that probably an MLP with fewer nodes would not improve but would not make the prediction much worse either.

Table 6.3: Number of nodes in each layer of each MISO-MLP model

Layers	MISO-MLP$_{H_2CO_3}$	MISO-MLP$_{NH_4^+}$	MISO-MLP$_{NH_3}$
Input	4	3	3
Normalization	3	3	3
Dense$_1$	32	64	128
Dense$_2$	32	0	0
Dropout	0	64	128
Output	1	1	1

The predictions of the industrial data using the MISO-MLP models are shown in Figure 6.5. The predicted values of ammonia concentration seem to be closer to the real data compared with ammonium predictions, which is unexpected. The predicted c$_{H_2CO_3}$ followed the same trend as the other concentrations for the first few samples, which means that the model could not extract enough information from the features on those points.

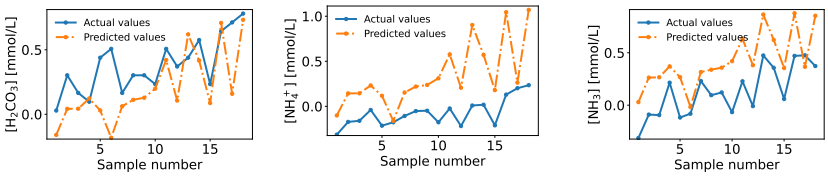

(a) Prediction of $c^T_{H_2CO_3}$ **(b)** Prediction of $c^T_{NH_4^+}$ **(c)** Prediction of $c^T_{NH_3}$

Figure 6.5: Predictions of industrial data using the MISO-MLP models

6.6 Discussion

The prediction of ammonia was revealed to be much harder than that of ammonium, resulting in a poor prediction of that variable. This might be due to the noise of the input variables that affects the ammonia concentration a lot, as its magnitude is much smaller. This effect does not disappear after preprocessing the data; it expands instead, as the magnitude after normalization is approximately 1000 times higher.

The MISO-MLP models gave the best performance due to different input features to each model, as adding not-so-important features can make NAS more complex and add a lot of useless cases, as happened with the MIMO-MLP model which showed slightly biased results, especially for ammonia concentration. This could be solved by increasing the maximum number of trials at the NAS step, but it would take longer, and would still have the possibility of finding different local minima, for better or worse.

6.7 Conclusion

The measurement of key waste products is not always easy to collect in real-time or at a required frequency, which reduces the possibility of stabilizing and optimizing the water quality for the fish. This can be improved by using machine learning models, such as multilayer perceptron.

The MLP models trained in this work are deep neural networks, and their architectures were optimized using an automated neural architecture search and tuning of hyperparameters. Three configurations were compared: MISO-MLPs; hybrid model; and MIMO-MLP. The best configuration was the MISO-MLP models together, although their performance was not so good. This might be due to the possibility of NAS reaching a local minimum or that the models could not capture the information from the training data, so a different type of model could perform better. A soft sensor using these models for monitoring would

perform better than the hybrid model, and the MIMO-MLP model, and could also complement the manual measurements, when estimating dissolved CO_2 and NH_3 concentrations.

6.8 Discussion of Paper III - Soft Sensor of Key Components in Recirculating Aquaculture Systems, using Feedforward Neural Networks

This chapter described the application of an automatic neural architecture search tool, named Auto-keras, in Python. This tool generates deep feedforward neural networks. The results of the last chapter showed that this type of neural network could not extract steady-state information from the input data. This might be due to the large amount of information on the input features, *i.e.*, large variability on the output variables, even though the features were not exactly the same for the MISO-MLP models.

One should note that the variation of the parameter gas-liquid ratio instead of the bypass fraction of the stripper air inlet causes the same effect of varying the stripper efficiency.

Chapter 7

Conclusions and Suggestions for Future Work

7.1 Conclusions

The recirculating aquaculture system has an inherent characteristic of being easier to maintain the conditions at a desired level, contributing to the fish welfare, than other types of aquaculture processes because it is in a closed environment and most of the water is recirculated. The recirculation flow conditions have the potential to be optimally controlled by automation instruments. In order to achieve this, in this thesis, we developed a model that is simple enough to be used for this purpose.

In the development phase, different types of models were tested. The extent of reactions approach was proven to have numerical issues. The biofilter was modelled as a CSTR and the ammonia conversion was considered to be constant. This is a valid assumption for the studied case, where the mass concentration of TAN is between 0.1 and 0.5 mg/L, although the same is not true when the concentration is higher than that, then the Monod model would be more adequate.

A good operating condition range is expected to make the effect of feeding on the fish metabolism insignificant. Within this range and assuming that the daily required amount of feed is provided, the fish metabolism is considered constant and described by reaction (3.1). This way, one can easily correct it when the fish's life cycle or the feed composition changes.

The developed models were used to design three control structures. Two of the three consisted of an optimization layer on top of proportional-integral (PI) control loops or nonlinear model-based predictive control (NMPC). A third structure consisted of a single layer with an economic NMPC (E-NMPC). This

part of the study presented how powerful can be the connection between RAS and advanced process control by applying a systematic procedure for developing PI control structures with steady-state optimal setpoints and comparing it with standard NMPC and E-NMPC frameworks. The control structures showed good performance after a transition period of two days except for the PI structure which caused out-of-bounds response of some variables. This transition period was mainly because the initial conditions were too far from the optimum.

The feedforward neural network application was developed in an attempt to predict concentrations that are not so often measured in the RAS facility where the test data came from. In the absence of real-time sampling, data-driven models can be used to aid monitoring and decision-making of variables that are hard to measure or not measured at all, considering more reliable and more frequently sampled data (twice a day would improve the model already).

7.2 Suggestions for Future Work

7.2.1 Continuous simulation

The next step of this study would be the development of an application to simulate the system continuously to help monitor the fish's performance. This would give a better visualization of dynamic responses of what to expect from changes in input variables.

7.2.2 Addition of feeding control

The absence of impact of feed on fish performance holds true under typical conditions. However, its reliability falters when unexpected events occur, like increased turbidity negatively affecting fish performance. A potential solution lies in implementing feeding controls, but a more robust approach involves exploring alternative performance metrics, such as image analysis, to identify suitable control variables for better adaptability.

7.2.3 Stripper model

In this work, the stripper modelled as a single-stage equilibrium column is fit for the optimal control application due to its simplicity. A suggestion for future work is to consider a more detailed model, for example, the model developed by Colt et al. (2012a).

7.2.4 Growth model

The main objective of optimizing the process is to maximize fish growth. Growth modeling in RAS is essential for understanding and optimizing the growth and production of fish, while taking into account both environmental conditions (temperature, pH, CO_2 and NH_3 concentrations, etc.) and the composition of the food. They are used to predict how various factors, such as water quality, feeding, stocking density, and temperature, impact the growth of fish. Incorporating this into the water quality model is a very challenging task.

7.2.5 Surrogate models

Chapter 6 studied the application of an automatic search tool to fit a feedforward neural network (FNN) to aid monitoring and decision-making in the absence of control or any fancier visualization technology to analyze fish performance, such as using image analysis approach. A suggestion remains to improve the study on the input features of the model. Another suggestion is to evaluate the use of other types of surrogate functions, for example, Gaussian process models.

Appendix A

Complementary material for Chapter 3

Derivation of Eq. (3.30)

Eq. (3.30) is used to compute pH as a function of the concentrations of the reaction invariants (TAN, TIC, and alkalinity). Comparing Eq. (3.30) with the equivalent equation in Henson and Seborg (1994), an extra term for TAN is added, which is caused by the contribution of NH_3 in the alkalinity definition.

Recall from Eq. (3.11) that the alkalinity is defined as:

$$c_{alk} = c_{OH^-} + c_{HCO_3^-} + 2c_{CO_3^{2-}} - c_{H^+} + c_{NH_3} \tag{A.1}$$

To derive Eq. (3.30), we need expressions for each species concentration as a function of c_{H^+} and the reaction invariants. First, we have that $c_{OH^-} = K_w/c_{H^+}$.

For the carbonate system, the equilibrium reactions and the definition of TIC concentration give:

$$c_{HCO_3^-} = K_1 \frac{c_{H_2CO_3}}{c_{H^+}} \tag{A.2}$$

$$c_{CO_3^{2-}} = K_2 \frac{c_{HCO_3^-}}{c_{H^+}} = K_1 K_2 \frac{c_{H_2CO_3}}{(c_{H^+})^2} \tag{A.3}$$

$$c_{TIC} = c_{H_2CO_3} + c_{HCO_3^-} + c_{CO_3^{2-}} \tag{A.4}$$

Combining Eqs. (A.2)-(A.4) gives:

$$c_{H_2CO_3} = c_{TIC}\left(1 + \frac{K_1}{c_{H^+}} + \frac{K_1K_2}{(c_{H^+})^2}\right)^{-1} \tag{A.5}$$

$$c_{HCO_3^-} = c_{TIC}\frac{K_1}{c_{H^+}}\left(1 + \frac{K_1}{c_{H^+}} + \frac{K_1K_2}{(c_{H^+})^2}\right)^{-1} \tag{A.6}$$

$$c_{CO_3^{2-}} = c_{TIC}\frac{K_1K_2}{(c_{H^+})^2}\left(1 + \frac{K_1}{c_{H^+}} + \frac{K_1K_2}{(c_{H^+})^2}\right)^{-1} \tag{A.7}$$

For ammonium, the ammonia-ammonium equilibrium reaction and the definition of TAN concentration give:

$$c_{NH_3} = K_3\frac{c_{NH_4^+}}{c_{H^+}} \tag{A.8}$$

$$c_{TAN} = c_{NH_3} + c_{NH_4^+} \tag{A.9}$$

Combining Eqs. (A.8) and (A.9) gives:

$$c_{NH_3} = K_3\frac{c_{TAN}}{c_{H^+}}\left(1 + \frac{K_3}{c_{H^+}}\right)^{-1} = c_{TAN}\frac{K_3}{c_{H^+} + K_3} \tag{A.10}$$

Substituting these expressions into the definition of alkalinity in Eq. (A.1) gives:

$$\begin{aligned} c_{alk} = \frac{K_w}{c_{H^+}} + c_{TIC}\left(1 + \frac{K_1}{c_{H^+}} + \frac{K_1K_2}{(c_{H^+})^2}\right)^{-1}\left(\frac{K_1}{c_{H^+}} + 2\frac{K_1K_2}{(c_{H^+})^2}\right) \\ - c_{H^+} + c_{TAN}\frac{K_3}{c_{H^+} + K_3} \end{aligned} \tag{A.11}$$

or

$$\begin{aligned} c_{alk} = c_{TIC}\frac{K_1c_{H^+} + 2K_1K_2}{(c_{H^+})^2 + K_1c_{H^+} + K_1K_2} + \frac{K_w}{c_{H^+}} - c_{H^+} \\ + c_{TAN}\frac{K_3}{c_{H^+} + K_3} \end{aligned} \tag{A.12}$$

which is the desired expression (3.30).

Phosphate. The expression in (A.12) may be extended to include other acids or bases. Specifically, if we include phosphate in the system, which is common in wastewater treatment systems, a fourth reaction invariant is needed, namely total phosphorus (TP),

$$c_{TP} = c_{H_3PO_4} + c_{H_2PO_4^-} + c_{HPO_4^{2-}} + c_{PO_4^{3-}} \tag{A.13}$$

Additional terms must be added to the alkalinity definition to account for $H_2PO_4^-$, HPO_4^{2-}, and PO_4^{3-} contributions. From atomic balances, the alkalinity with phosphate included becomes:

$$c_{alk} = c_{OH^-} + c_{HCO_3^-} + 2c_{CO_3^{2-}} - c_{H^+} + c_{NH_3} + c_{H_2PO_4^-} + 2c_{HPO_4^{2-}} + 3c_{PO_4^{3-}} \tag{A.14}$$

For the phosphate system, we have, from its three equilibrium reactions:

$$c_{H_2PO_4^-} = K_4 \frac{c_{H_3PO_4}}{c_{H^+}} \tag{A.15}$$

$$c_{HPO_4^{2-}} = K_5 \frac{c_{H_2PO_4^-}}{c_{H^+}} \tag{A.16}$$

$$c_{PO_4^{3-}} = K_6 \frac{c_{HPO_4^{2-}}}{c_{H^+}} \tag{A.17}$$

Combining the definition of TP in Eq. (A.13) with Eqs. (A.15)-(A.17) gives the following expression for the three contributions from phosphate to alkalinity (c_{alk}):

$$c_{H_2PO_4^-} + 2c_{HPO_4^{2-}} + 3c_{PO_4^{3-}} = c_{TP} \frac{K_4(c_{H^+})^2 + 2K_4K_5c_{H^+} + 3K_4K_5K_6}{(c_{H^+})^3 + K_4(c_{H^+})^2 + K_4K_5c_{H^+} + K_4K_5K_6} \tag{A.18}$$

Eq. (A.18) needs to be added to the right-hand side of Eq. (A.12) and the resulting expression for c_{alk} can be used to compute pH (*i.e.*, c_{H^+}) as a function of TIC, TAN, TP, and alkalinity. The phosphoric acid concentration is then given by:

$$c_{H_3PO_4} = c_{TP} \left(1 + \frac{K_4}{c_{H^+}} + \frac{K_4K_5}{(c_{H^+})^2} + \frac{K_4K_5K_6}{(c_{H^+})^3}\right)^{-1} \tag{A.19}$$

References

Andersson, J.A., Gillis, J., Horn, G., Rawlings, J.B., and Diehl, M. (2019). CasADi: a software framework for nonlinear optimization and optimal control. *Mathematical Programming Computation*, 11(1), 1–36. doi:10.1007/s12532-018-0139-4.

Bandura, A.V. and Lvov, S.N. (2006). The ionization constant of water over wide ranges of temperature and density. *Journal of Physical and Chemical Reference Data*, 35(1), 15–30. doi:10.1063/1.1928231.

Barbu, M., Ceangă, E., and Caraman, S. (2016). Water Quality Modeling and Control in Recirculating Aquaculture Systems. *Urban Agriculture*. doi:10.5772/62302. URL https://www.intechopen.com/chapters/50109.

Benson, B.B. and Krause, D. (1984). The concentration and isotopic fractionation of oxygen dissolved in freshwater and seawater in equilibrium with the atmosphere. *Limnology and Oceanography*, 29(3), 620–632. doi:10.4319/lo.1984.29.3.0620.

Bergheim, A. and Fivelstad, S. (2014). Atlantic Salmon (Salmo Salar L.) in aquaculture: Metabolic rate and water flow requirements. In *Salmon: Biology, Ecological Impacts and Economic Importance*, chapter 8, 155–171. Nova Publishers Inc., New York, USA.

BLUEGREEN GROUP (2022). FiiZK // Intake pipe for closed cage. URL https://bluegreengroup.no/en/about-us/news/fiizk-intake-pipe-for-closed-cage.

California Institute of Technology (2021). Carbon Dioxide - Vital Signs - Climate Change: Vital Signs of the Planet. URL https://climate.nasa.gov/vital-signs/carbon-dioxide/.

Colt, J., Watten, B., and Pfeiffer, T. (2012a). Aquacultural Engineering Carbon

dioxide stripping in aquaculture – Part II : Development of gas transfer models. *Aquacultural Engineering*, 47, 38–46. doi:10.1016/j.aquaeng.2011.12.002.

Colt, J., Watten, B., and Pfeiffer, T. (2012b). Carbon dioxide stripping in aquaculture - Part III: Model verification. *Aquacultural Engineering*, 47, 47–59. doi:10.1016/j.aquaeng.2011.12.007. URL http://dx.doi.org/10.1016/j.aquaeng.2011.12.007.

Cripps, S.J. and Bergheim, A. (2000). Solids management and removal for intensive land-based aquaculture production systems. *Aquacultural Engineering*, 22(1-2), 33–56. doi:10.1016/S0144-8609(00)00031-5.

Davidson, J., Good, C., Williams, C., and Summerfelt, S.T. (2017). Evaluating the chronic effects of nitrate on the health and performance of post-smolt Atlantic salmon Salmo salar in freshwater recirculation aquaculture systems. *Aquacultural Engineering*, 79, 1–8. doi:10.1016/J.AQUAENG.2017.08.003.

dos Santos, A.M., Bernardino, L.F., Attramadal, K.J., and Skogestad, S. (2023). Steady-state and dynamic model for recirculating aquaculture systems with pH included. *Aquacultural Engineering*, 102, 14. doi:10.1016/J.AQUAENG.2023.102346.

European Market Observatory for Fisheries and Aquaculture Products (2021). *Freshwater aquaculture in the EU*. March. European Union. doi:10.2771/594002.

FAO (2020). The State of World Fisheries and Aquaculture 2020. Technical report, FAO, Rome. doi:https://doi.org/10.4060/ca9229en.

FAO (2022). The State of World Fisheries and Aquaculture 2022. Technical report, FAO, Rome, Italy. doi:10.4060/CC0461EN.

Farghally, H.M., Atia, D.M., El-madany, H.T., and Fahmy, F.H. (2014). Control methodologies based on geothermal recirculating aquaculture system. *Energy*, 78, 826–833. doi:10.1016/j.energy.2014.10.077.

Farheen, U., Preeti, H.M., and Dr.BaswarajGadgay (2018). Automatic Controlling of Fish Feeding System. *International Journal for Research in Applied Science and Engineering Technology*, 6(7), 362–366. doi:10.22214/ijraset.2018.7050.

Farmasino CO. LTD (2021). Factory supply high quality 99% Sodium bicarbonate/Natrium Bicarbonate/Bicarbonate/NaHCO3 of Soda cas 144-55-8.

Fortuna, L., Graziani, S., Rizzo, A., and Xibilia, M.G. (2007). *Soft Sensors for Monitoring and Control of Industrial Processes (Advances in Industrial Control)*. Springer-Verlag London.

Frazer, L.N. (2009). Sea-Cage Aquaculture, Sea Lice, and Declines of Wild Fish. *Conservation Biology*, 23(3), 599–607. doi:10.1111/J.1523-1739.2008.01128.X.

Global Salmon Initiative (2020). About Salmon Farming. URL https://globalsalmoninitiative.org/en/about-salmon-farming/.

Gustafsson, T.K. and Waller, K.V. (1983). Dynamic modeling and reaction invariant control of pH. *Chemical Engineering Science*, 38(3), 389–398. doi:10.1016/0009-2509(83)80157-2.

Hatchery - Feed & Management (2020). Sweden plans 100,000 ton salmon RAS farm. URL https://hatcheryfm.com/news/latest-news/sweden-plans-100000-ton-salmon-ras-farm/.

Henson, M.A. and Seborg, D.E. (1994). Adaptive Nonlinear Control of a pH Neutralization Process. *IEEE Transactions on Control Systems Technology*, 2(3), 169–182.

Hindmarsh, A.C., Brown, P.N., Grant, K.E., Lee, S.L., Serban, R., Shumaker, D.E., and Woodward, C.S. (2005). SUNDIALS: Suite of nonlinear and differential/algebraic equation solvers. *ACM Transactions on Mathematical Software*, 31(3), 363–396. doi:10.1145/1089014.1089020.

Hornik, K., Stinchcombe, M., and White, H. (1989). Multilayer feedforward networks are universal approximators. *Neural Networks*, 2(5), 359–366. doi:10.1016/0893-6080(89)90020-8.

Jin, H., Song, Q., and Hu, X. (2018). Auto-Keras: An Efficient Neural Architecture Search System. *Proceedings of the ACM SIGKDD International Conference on Knowledge Discovery and Data Mining*, 1946–1956. doi:10.1145/3292500.3330648.

Jin, R., Chen, W., and Sudjianto, A. (2005). An efficient algorithm for constructing optimal design of computer experiments. *Journal of Statistical Planning and Inference*, 134(1), 268–287. doi:10.1016/J.JSPI.2004.02.014.

Johansson, O. and Wedborg, M. (1980). The ammonia-ammonium equilibrium in seawater at temperatures between 5 and 25°C. *Journal of Solution Chemistry*, 9(1), 37–44. doi:10.1007/BF00650135.

Khan, J.R., Johansen, D., and Skov, P.V. (2018). The effects of acute and long-term exposure to CO2 on the respiratory physiology and production performance of Atlantic salmon (Salmo salar) in freshwater. *Aquaculture*, 491, 20–27. doi: 10.1016/J.AQUACULTURE.2018.03.010.

Lee, J., Angani, A., Thalluri, T., and Shin, K.J. (2020). Realization of water process control for smart fish farm. *2020 International Conference on Electronics, Information, and Communication, ICEIC 2020*. doi:10.1109/ICEIC49074.2020.9051285.

Lembo, G. and Mente, E. (eds.) (2019). *Organic Aquaculture. Impacts and future developments*. Springer Cham, 1 edition. doi:10.1007/978-3-030-05603-2.

Li, W., Cheng, X., Xie, J., Wang, Z., and Yu, D. (2019). Hydrodynamics of an in-pond raceway system with an aeration plug-flow device for application in aquaculture: an experimental study. *Royal Society Open Science*, 6(7). doi: 10.1098/RSOS.182061. URL https://royalsocietypublishing.org/doi/10.1098/rsos.182061.

Liu, Z., Li, X., Fan, L., Lu, H., Liu, L., and Liu, Y. (2014). Measuring feeding activity of fish in RAS using computer vision. *Aquacultural Engineering*, 60, 20–27. doi:10.1016/J.AQUAENG.2014.03.005.

Malone, R.F., Bergeron, J., and Cristina, C.M. (2006). Linear versus Monod representation of ammonia oxidation rates in oligotrophic recirculating aquaculture systems. *Aquacultural Engineering*, 34(3), 214–223. doi:10.1016/J.AQUAENG.2005.08.005.

Millero, F.J. and Huang, F. (2009). The density of seawater as a function of salinity (5 to 70 g kg-1) and temperature (273.15 to 363.15 K). *Ocean Science*, 5(2), 91–100. doi:10.5194/os-5-91-2009.

Millero, F.J., Graham, T.B., Huang, F., Bustos-Serrano, H., and Pierrot, D. (2006). Dissociation constants of carbonic acid in seawater as a function of salinity and temperature. *Marine Chemistry*, 100(1-2), 80–94. doi:10.1016/j.marchem.2005.12.001.

Mota, V.C., Nilsen, T.O., Gerwins, J., Gallo, M., Ytteborg, E., Baeverfjord, G., Kolarevic, J., Summerfelt, S.T., and Terjesen, B.F. (2019). The effects of carbon dioxide on growth performance, welfare, and health of Atlantic salmon post-smolt (Salmo salar) in recirculating aquaculture systems. *Aquaculture*, 498(March 2018), 578–586. doi:10.1016/j.aquaculture.2018.08.075.

Nistad, A.A. (2018). Energy use and efficiency in recirculating aquaculture systems. Technical report, Norwegian University of Science and Technology, NTNU, Trondheim.

Pedersen, S. (2018). *Simulation and Optimization of Recirculating Aquaculture Systems*. Ph.D. thesis, Chalmers University of Technology.

Pedersen, S. and Wik, T. (2020). A comparison of topologies in recirculating aquaculture systems using simulation and optimization. *Aquacultural Engineering*, 89, 102059. doi:10.1016/j.aquaeng.2020.102059.

Rabanal, H.R. (1988). History of aquaculture. URL http://www.fao.org/docrep/field/009/ag158e/AG158E02.htm.

Raoeliaritiana, J.O. (2016). *Methods for determining the activity of nitrifying bacteria in wastewater samples*. Ph.D. thesis, University of Stavanger.

Ridler, N.B. and Hishamunda, N. (2001). Promotion of sustainable commercial aquaculture in sub-Saharan Africa. Technical report, Food and Agriculture Organization of the United Nations, Rome.

Schreier, H.J., Mirzoyan, N., and Saito, K. (2010). Microbial diversity of biological filters in recirculating aquaculture systems. *Current Opinion in Biotechnology*, 21(3), 318–325. doi:10.1016/j.copbio.2010.03.011.

Skogestad, S. (2003). Simple analytic rules for model reduction and PID controller tuning. *Journal of Process Control*, 13(4), 291–309. doi:10.1016/S0959-1524(02)00062-8.

Summerfelt, R.C. and Penne, C.R. (2005). Solids removal in a recirculating aquaculture system where the majority of flow bypasses the microscreen filter. *Aquacultural Engineering*, 33(3), 214–224. doi:10.1016/j.aquaeng.2005.02.003.

Summerfelt, S.T., Vinci, B.J., and Piedrahita, R.H. (2000). Oxygenation and carbon dioxide control in water reuse systems. *Aquacultural Engineering*, 22(1-2), 87–108. doi:10.1016/S0144-8609(00)00034-0.

Summerfelt, S.T., Mathisen, F., Holan, A.B., and Terjesen, B.F. (2016). Survey of large circular and octagonal tanks operated at Norwegian commercial smolt and post-smolt sites. *Aquacultural Engineering*, 74, 105–110. doi:10.1016/j.aquaeng.2016.07.004.

Summerfelt, S.T., Zühlke, A., Kolarevic, J., Reiten, B.K.M., Selset, R., Gutierrez, X., and Terjesen, B.F. (2015). Effects of alkalinity on ammonia removal, carbon dioxide stripping, and system pH in semi-commercial scale water recirculating aquaculture systems operated with moving bed bioreactors. *Aquacultural Engineering*, 65, 46–54. doi:10.1016/j.aquaeng.2014.11.002.

Tal, Y., Schreier, H.J., Sowers, K.R., Stubblefield, J.D., Place, A.R., and Zohar, Y. (2009). Environmentally sustainable land-based marine aquaculture. *Aquaculture*, 286(1-2), 28–35. doi:10.1016/J.AQUACULTURE.2008.08.043.

Thorarensen, H. and Farrell, A.P. (2011). The biological requirements for post-smolt Atlantic salmon in closed-containment systems. *Aquaculture*, 312(1-4), 1–14. doi:10.1016/J.AQUACULTURE.2010.11.043.

Tianjin Chengyuan Chemical CO. LTD (2021). Caustic soda flakes 99%.

Tidwell, J.H. (ed.) (2012). *Aquaculture Production Systems*. John Wiley & Sons. doi:10.1002/9781118250105.

Trondheim kommune (2021). Vann og avløp for innbygger.

Villar-Navarro, E., Garrido-Pérez, C., and Perales, J.A. (2021). The potential of different marine microalgae species to recycle nutrients from recirculating aquaculture systems (RAS) fish farms and produce feed additives. *Algal Research*, 58, 102389. doi:10.1016/J.ALGAL.2021.102389.

Vinci, B.J., Timmons, M.B., Summerfelt, S.T., and Watten, B.J. (1996). Carbon Dioxide Control in Intensive Aquaculture: Design Tool Development. In *Aquacultural Engineering Society Proceedings*, 226–244.

Weiss, R.F. (1974). Carbon dioxide in water and seawater: the solubility of a non-ideal gas. *Marine Chemistry*, 2(3), 203–215. doi:10.1016/0304-4203(74)90015-2.

Werbos, P.J. (1974). *Beyond Regression : New Tools for Prediction and Analysis in the Behavioral Sciences*. Ph.D. thesis, Harvard University.

Wik, T.E., Lindén, B.T., and Wramner, P.I. (2009). Integrated dynamic aquaculture and wastewater treatment modelling for recirculating aquaculture systems. *Aquaculture*, 287(3-4), 361–370. doi:10.1016/j.aquaculture.2008.10.056.

Wright, J.P. (2011). *pH Control in Recirculating Aquaculture Systems for Pāua (Haliotis iris)*. Ph.D. thesis, Victoria University of Wellington.